ANALYSIS OF MOUNT SEMERU EXPLOSION USING MULTI-SENSOR REMOTE SENSING DATA IN 2021-2022

UNDERGRADUATE THESIS

Submitted for the Bachelor's Degree Examination in the

Geophysics Study Program Faculty of Mathematics and Natural Sciences

Universitas Padjadjaran

RANIA ALIFA DESENALDO

140710190039

GEOPHYSICS STUDY PROGRAM

FACULTY OF MATHEMATICS AND NATURAL SCIENCES

UNIVERSITAS PADJADJARAN

2023

APPROVAL SHEET

TITLE	:	ANALYSIS OF MOUNT SEMERU EXPLOSION USING MULTI-SENSOR REMOTE SENSING DATA IN 2021-2022
AUTHOR	:	RANIA ALIFA DESENALDO
NPM	:	140710190039

Bandung, February 2023

Approved,

Main Supervisor	Co-Supervisor
Dr. Irwan Ary Dharmawan	**Muhammad Aufaristama, Ph.D.**
NIP. 19720531 199702 1 001	**NIP. -**

Known by,

Head of Geophysics Study Program

Faculty of Mathematics and Natural Sciences

Universitas Padjadjaran

Dr. Irwan Ary Dharmawan

NIP. 19720531 199702 1 001

This thesis is dedicated to my Papa and Mama,

who have always provided ice, support, and unconditional love,

to Teh Rana who has always been a great listener

and a fun chat buddy every day,

and also to my 30 cats at home

who have been my playmates, helping me avoid boredom and stress

during the thesis work.

PREFACE

Praises and thanks are offered to Allah SWT for His grace, blessings, guidance, as well as the opportunities and health bestowed upon the author, enabling the completion of the thesis titled **“ANALYSIS OF MOUNT SEMERU EXPLOSION USING MULTI-SENSOR REMOTE SENSING DATA IN 2021-2022”**. This thesis is one of the requirements for the Bachelor's degree examination in the Geophysics Study Program, Faculty of Mathematics and Natural Sciences, Universitas Padjadjaran.

The preparation of this thesis could not have been accomplished without the assistance of various parties. Therefore, the author would like to express heartfelt gratitude to all those who have contributed to the process of preparing this thesis, including:

1. Dr. Irwan Ary Dharmawan, as the main supervisor, for the guidance and invaluable input, advice, and direction provided throughout the thesis process, and to Muhammad Aufaristama Ph.D., as the co-supervisor, for consistently assisting and answering all the author's technical questions during the thesis work,
2. Prof. Dr. rer. nat. Yudi Rosandi, M.Si., and Dr. Imran Hilman Mohammad, as the reviewers and examiners, for providing input and suggestions for the thesis writing,

3. Dr. Kartika Hajar Kirana S.Pd., as the comprehensive examiner, who guided the author during the examination and provided valuable input on the thesis material,
4. Pak Kusna, Bu Leo, Bu Dini, Pak Asep, Pak Eddy, and other Geophysics lecturers at Unpad who provided instruction to the author throughout seven semesters,
5. Bu Veni, Pak Didit, Pak Pena, Pak Ia, Pak Oos, Bu Uci, Pak Deni, Pak Alex, and other educational staff of Geophysics at Unpad who consistently assisted and facilitated the author's learning process during their time on campus,
6. Fina, Fitria, and Aida, as the author's closest friends since the first semester, who always shared stories, joys, sorrows, moments, and support throughout their academic journey, including the thesis work,
7. Tubagus, Dhiyya, and Aristo, as fellow comrades in Remote Sensing Final Project, providing a space for discussion and sharing experiences during the thesis process,
8. Catherine, Wadi, and Tubagus, fellow members of the Jagawana Padjadjaran project, who consistently supported and provided the best discussions throughout their academic journey,
9. Farah, Alif, Randy, Fina, and Fitria, fellow laboratory assistants in Geophysical Instrumentation and Signal Processing, who always brought laughter and entertainment to the author during the thesis work,

10. Safhira, Dita, Muti, Zhilal, Abib, and other fellow students from the 2019 class of Geophysics Unpad Rangsatierra, who accompanied the author throughout their studies and thesis writing.

The author acknowledges that there are still many shortcomings in the preparation of this thesis, and the author is very open to criticism, suggestions, and input to improve the research. The author hopes that this thesis can be beneficial to anyone who reads it. Amen.

February 2023

ABSTRACT

Mount Semeru erupted on December 4th, 2021, was one of the biggest eruptions in its history. This event brings different opinion regarding the cause of the eruption, whether due to internal (magmatic) or external (collapse) factor. Observation through morphological (lava dome), thermal, and precipitation parameters using remote sensing method in 2021-2022 were done to determine the cause of eruption. There were several eruptions occurred before December 2021 detected by thermal anomaly (threshold above 50°C) although lava dome area has not changed significantly. Precipitation has also increased by 77% during October-November 2021. When the eruption occurred in December 2021, lava dome area decreased by 81%, but the thermal anomaly area and precipitation values tended to be high. After the eruption, lava dome began to form again and there were several months still experienced eruptions. Based on these results, it is indicated that the eruption of Mount Semeru occurred due to external factor (collapse) based on a decrease in lava dome area, an increase in thermal anomalies area, and an increase in precipitation values. For further research, high-resolution temporal remote sensing and seismic data are needed to see whether the collapse caused by external or internal factor on December 2021 anomaly.

Keywords: Mount Semeru, remote sensing, morphology, thermal, precipitation

TABLE OF CONTENTS

LIST OF TABLES

LIST OF FIGURES

CHAPTER I

INTRODUCTION

1.1 Research Background

Mount Semeru is the highest stratovolcano on the island of Java, located in the Lumajang and Malang regencies of East Java. Its peak, known as Mahameru, stands at an elevation of 3,676 meters above sea level, while the lava dome or crater named Jonggring Seloko reaches an elevation of 3,744.5 meters above sea level. The mountain is surrounded by fertile agricultural land, and there are settlements on its eastern and southeastern slopes. The natural resources around Mount Semeru are utilized for sand and stone mining along the Rejali River, Regoyo River, and Glidig River (Geologi, 2014).

Mount Semeru first experienced an eruption on November 8, 1818, as recorded in history. The mountain began to show renewed activity from 1829 to 1993, mostly characterized by lava flows, lahars, pyroclastic flows, and damage to cultivated land. The largest eruption occurred from February 2 to 15, 1994, during which thick white smoke, lava flows, and tremors were observed for seven days. There were reports of loud explosions followed by ashfall and pyroclastic flows resulting from the lava flows. This event claimed the lives of seven people who were struck by pyroclastic flows and two individuals who were swept away by lahars. Another significant eruption occurred from March 11 to December 29, 2002, marked by increased shallow and deep volcanic earthquakes, tremors, incandescent lava flows, pyroclastic flows, and seven eruptions in the main crater. This event did not result in any loss of life or damage to facilities around Mount Semeru. Subsequent volcanic activity was reported in 2004, 2005, 2007, 2008, 2009, and up until 2020 (Geologi, 2014). Recently, Mount Semeru has once again exhibited activity with its latest eruption.

On December 4, 2021, Mount Semeru erupted, releasing a pyroclastic flow cloud reaching a height of 11 kilometers that headed towards the Pronojiwo and Sumberwuluh districts in Lumajang, East Java. This eruption also resulted in pyroclastic material explosions and ashfall-induced lahars. Additionally, there were reports of rockfalls, blast earthquakes, deep volcanic earthquakes, and distant tectonic earthquakes that damaged hundreds of buildings, houses, transportation networks, farmland, and caused loss of life (Prasetiawan, 2021). As of March 27, 2022, and October 2022, there has still been activity at Mount Semeru, with an ash column reaching 4,676 meters above sea level recorded by seismographs, with a maximum amplitude of 20 mm and a duration of 294 seconds (Pura, 2022).

According to M. Haris Miftakhul Fajar, a Geological expert from Institut Teknologi Sepuluh Nopember (ITS) (Aprillya, 2021), the eruption of Mount Semeru was caused by the accumulation of previous eruptions in the days leading up to it. The eruption was due to internal factors (magmatic), resulting from the instability of the magma chamber. Based on data from Pusat Vulkanologi dan Mitigasi Bencana Geologi (PVMBG), there was volcanic activity associated with the eruption of Mount Semeru, as evidenced by seismic data recordings showing small-intensity eruption earthquakes, even though there were no signs of earthquakes on the day of the eruption. However, according to Mirzam

Abdurrachman, a Volcanology expert from Institut Teknologi Bandung (ITB) (Aprillya, 2021), the eruption of Mount Semeru was caused by a landslide above the magma chamber. This occurred due to heavy rainfall, causing a significant amount of water to enter the cracks in the lava dome and react with materials inside the mountain. Additionally, volcanic ash materials covering the mountain's summit were eroded by the water. This resulted in the removal of the load covering the summit of Mount Semeru, leading to an explosive eruption due to the interaction between water and magma inside the mountain, even though the magma chamber was only partially filled (Permana, 2021). This event is referred to as an eruption caused by external factors (collapse), which led to the emergence of pyroclastic flows.

The existence of two different opinions regarding the cause of the Mount Semeru eruption in December 2021 has prompted further observation. Determining the conditions of this eruption is considered important for distinguishing between magmatic and non-magmatic eruptions, interpreting the types of rocks resulting from the eruption, simulating eruption flows, and other benefits. Initial observations have been conducted by Geological expert from Universitas Gadjah Mada (UGM), Haryo Edi Wibowo, using seismic methods and visual observations. However, it is necessary to observe volcanic activity using a combination of several other methods, such as morphological observations to identify the stability and growth of the lava body, and visual observations through thermal cameras to eliminate weather factors (Gloria, 2021). One of the methods that can support these observations is remote sensing.

Remote sensing is a method used to acquire information in the form of surface images of the Earth without direct contact with the objects being observed. This method typically involves satellites that capture images of the Earth's surface using sunlight as a source of illumination. The data from these captured images are stored in a server, allowing users to access the data freely (Sanderson, 2006). Some examples of using remote sensing methods in monitoring volcanic activity include thermal volcanic system observation in active Latin American volcanoes using sensors like ASTER and MODIS (Reath et al., 2018), reconstructing the eruption of Mount Fogo in 2014-2015 using thermal sensors like MODIS and SEVIRI (Miranda et al., 2022), and monitoring the morphological evolution of Mount Krakatau using SAR and optical remote sensing data (Xiang et al., 2022). These examples demonstrate that remote sensing methods are highly suitable for observing the morphology and thermal characteristics of volcanoes using multi-sensor satellites.

When a volcano erupts, there will inevitably be changes in morphology, especially in the lava dome (Walter et al., 2019). This eruption can also trigger a high temperature in the volcano due to magma activity rising to the surface (Plank et al., 2020). Therefore, observations of morphology and thermal changes are crucial as supporting data for seismic observations, visual observations, and indicators of eruptions caused by internal or magmatic factors. Rainfall observations are also necessary as a parameter to monitor external conditions around the volcano, considering the frequency of rain events before the eruption occurs. Rainfall data also serves as supporting evidence for eruptions caused by external factors or collapse (Farquharson and Amelung, 2019).

Therefore, morphology, thermal, and rainfall observations will be conducted on Mount Semeru in December 2021 using remote sensing methods and multi-sensor satellite data. The ultimate goal of these observations is expected to provide insights into whether the eruption that occurred falls under the category of internal (magmatic) or external (collapse) eruption phenomena.

1.2 Problem Identification

Due to the differences in opinion regarding the eruption of Mount Semeru, whether it is classified as an eruption or collapse event, the research questions underlying this study are as follows,

1. What were the processes occurring on Mount Semeru before and after the eruption in December 2021 based on morphological data?
2. What were the processes occurring on Mount Semeru before and after the eruption in December 2021 based on thermal data?
3. What were the processes occurring on Mount Semeru before and after the eruption in December 2021 based on observations of rainfall data?
4. Did Mount Semeru experience an eruption due to internal (magmatic) or external (collapse) factors?

1.3 Research Purpose and/or Objectives

The purpose of this research is to apply remote sensing methods using multi-sensor satellite data to map the morphology, thermal imagery, and rainfall data of Mount Semeru. The objective of this study is to generate maps and graphs of the morphological, thermal, and rainfall parameters that can provide insights into whether Mount Semeru experienced an eruption due to internal (magmatic) or external (collapse) factors.

1.4 Research Benefits

The results of this research can provide the following benefits:

1. Theoretical Benefits

This research is expected to serve as a reference for future studies related to observing the conditions that occurred at Mount Semeru using remote sensing visual observations. It can also broaden insights into the implementation of remote sensing methods in visualizing volcanic activities. Additionally, the research aims to differentiate between magmatic and non-magmatic eruptions, interpret the types of rocks resulting from eruptions, and simulate eruption flows.

2. Practical Benefits

a. For the author, this research is expected to serve as a means of sharing the author's knowledge in implementing remote sensing methods for observing Mount Semeru's conditions.

b. For researchers, this research is expected to provide supporting data during the monitoring process of Mount Semeru's activities, utilizing observations of morphology, moisture/water presence, thermal aspects, and rainfall from remote sensing satellite data.

1.5 Conceptual Framework

Mount Semeru is the tallest stratovolcano on the island of Java, located in Lumajang and Malang regencies, East Java. Mount Semeru erupted in December 2021, resulting in casualties and the destruction of hundreds of buildings. As of March 27 and October 2022, Mount Semeru's activities are still recorded through visual observations and seismographic instruments. Due to this eruption, the lava dome of Mount Semeru underwent changes in shape and size. Specifically, the conceptual framework is presented in Figure 1.1.

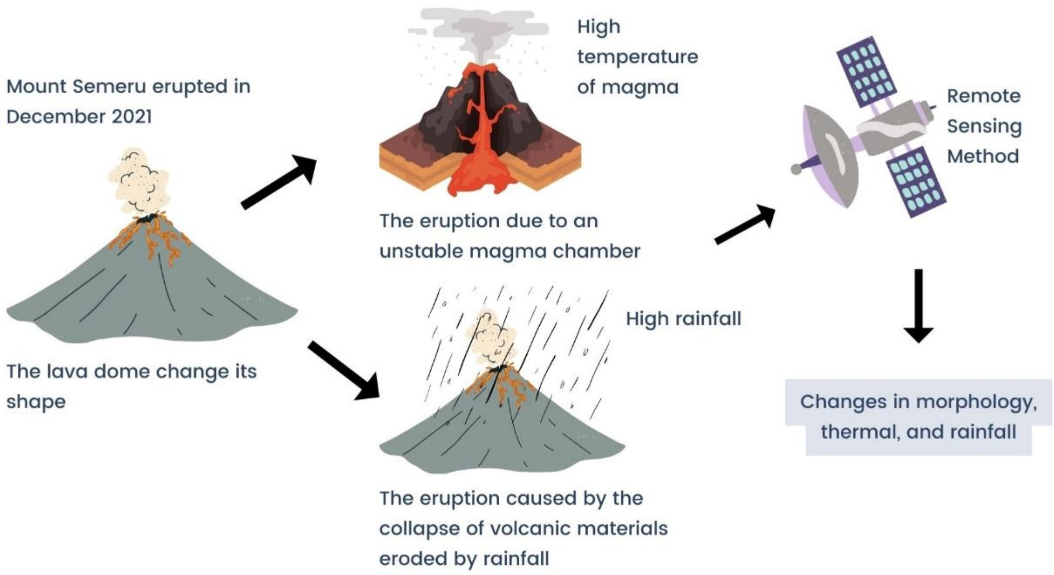

Figure 1.1 Conceptual Framework of the Research

The eruption has triggered several opinions regarding the condition of Mount Semeru, including whether it resulted from an internal (magmatic) eruption, which occurs when the conditions in the magma chamber are unstable, or an external (collapse) eruption, which occurs when volcanic material on the mountain's slopes is eroded by water. The internal (magmatic) factor is related to the condition of the magma inside the volcano, which experiences increased activity and high temperatures. On the other hand, the external (collapse) factor is linked to the erosion of volcanic materials by continuous rainfall, which has been detected as having high precipitation rates. Therefore, further observations are required, particularly through visual observations, focusing on morphology, thermal imaging, and rainfall data. This research aims to validate whether the eruption of Mount Semeru resulted from internal or external factors based on observations of morphology, thermal imagery, and rainfall data.

Research on the observation of morphology and thermal imagery in volcanoes has been conducted by Reath et al. (2018), Miranda et al. (2022), and Xiang et al. (2022) using remote sensing data from SAR and optical sensors for morphology and multi-sensor satellite data including ASTER, MODIS, and SEVIRI for thermal observations. The results indicate differences in morphology before and after eruptions, as well as the detection of increasingly hot thermal imagery accompanied by the appearance of hotspots after eruptions.

Therefore, multi-sensor satellite data from Planet NICFI were utilized for morphological observations, Landsat 8 satellite data for thermal imagery observations, and CHIRPS data for rainfall observations. The selection of these parameters was based on the observation needs related to morphology, thermal aspects, and rainfall, as well as the preliminary research that has been conducted.

Based on the initial hypothesis, an eruption due to internal factors may occur when there is an upward trend in thermal activity on the date of the eruption, supported by changes in the morphology of Mount Semeru. On the other hand, external factors may come into play when there is a high rainfall value, along with changes in the morphology of Mount Semeru's slopes.

1.6 Research Methodology

The method applied in this research is remote sensing, which can capture and record phenomena on the Earth's surface without direct physical contact. The data are recorded by multi-sensor satellites as the data source for each parameter and can be accessed through Google Earth Engine. Google Earth Engine serves as a platform for data preparation, data preprocessing, and data processing.

The first step carried out is preparing the data originating from a collection of satellite images. The satellites used include Planet NICFI for obtaining images representing morphology, Landsat 8 for acquiring thermal imagery, and CHIRPS data for rainfall imagery. The selection of these satellites is based on considerations such as spatial resolution, temporal resolution, and the suitability of each satellite in providing the required data.

The second stage involves data preprocessing. This stage is carried out to apply various types of filters to ensure that the satellite images exhibit the desired visualization. The applied filters include a cloud-free filter to remove cloud cover interference in the images, a location filter to limit observations to the research object, which is Mount Semeru, and a time filter to determine the start and end times of observations, which are in the years 2021-2022.

The third stage involves data processing, which entails processing all the images to generate morphology maps, thermal maps, and rainfall maps. All these maps can be obtained by selecting the appropriate bands and displaying them using color variations. Band selection is tailored to the parameters being used, which include morphology, thermal aspects, and rainfall. From these images, time series graphs can be generated to observe changes in morphology, thermal characteristics, and rainfall over time from 2021 to 2022.

1.7 Research Location and Time

The location of this research is in Mount Semeru, Lumajang and Malang Regency, East Java, Indonesia. This research is conducted in the Geophysics Study Program, Faculty of Mathematics and Natural Sciences, Universitas Padjadjaran.

This research was conducted over a period of five months, from August 2022 to January 2023. August 2022 was dedicated to literature review and data collection. September, October, and November 2022 were used for processing satellite imagery for each parameter, including morphology, thermal, and rainfall, along with the analysis of each image. In November 2022, data analysis of all processed images was conducted. Subsequently, December 2022 was used for data validation and evaluation, while January 2023 was used to complete the report and finalize all the stages that had been undertaken.

BAB II

LITERATURE REVIEW

2.1 General Description of Mount Semeru

Mount Semeru is a mountain located in Lumajang and Malang Regencies, East Java, at geographic coordinates of 08°06.5' S and 112°55' E. This mountain has other names such as Semeroe, Smeru, and Smiru, but the most commonly known and used name is Semeru. Mount Semeru belongs to the category of stratovolcanoes and has a peak known as Mahameru, which stands at an elevation of 3,676 meters above sea level, as well as a lava dome (crater) called Jonggring Seloko, which stands at an elevation of 3,744.5 meters above sea level. Due to its peak's height, it is often referred to as the tallest stratovolcano on the island of Java. Mount Semeru is situated in an area with fertile agricultural land, particularly to the east and southeast of the mountain, and this region is also populated, making it vulnerable to natural disasters (Geologi, 2014).

Mount Semeru has a morphology that resembles an imperfect cone but can appear more perfectly when viewed from the south and southeast, as illustrated in Figure 2.1. Its Mahameru crater is located on the northern side of the mountain, and it gradually extends towards the south and southeast. Mount Semeru is part of the same alignment as Mount Jambangan and the Tengger Mountains in a south-to-north direction. Its structure indicates the presence of faults, craters, maars, and calderas. These faults include normal faults oriented northwest-southeast, east-west, and northeast-southwest. The Mahameru crater, located at the summit of the

Semeru Mountain, is in the southeasternmost part of the mountain and is currently inactive. Another active crater is the Jonggring Seloko crater. This mountain also has five maars located along the complex of Mount Semeru up to Mount Jambangan, which is Ranu Pani, Ranu Regulo, Ranu Kumbolo, Ranu Pakis, and Ranu Darungan. The calderas on Mount Semeru, named Jambangan and Ajek-Ajek, have a floor, steep walls, and an old volcanic shape (Geologi, 2014).

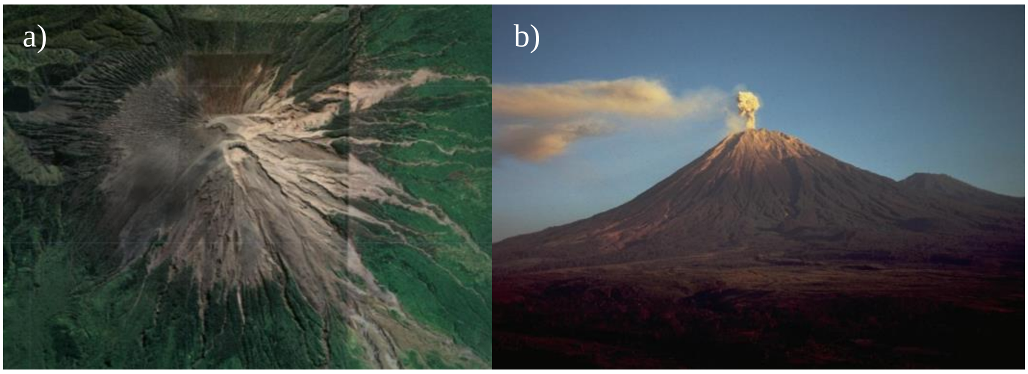

Figure 2.1 Mount Semeru from Google Earth Satellite Images (Last Updated in 2023). a) Mount Semeru Top View, b) Mount Semeru South-Southeast View (Global Volcanism Program, 2022)

The stratigraphic conditions on Mount Semeru result from eruptions at several eruption points. Based on the results of these eruptions, along with the lithology types and their stratigraphic positions, there are five rock groups on Mount Semeru, which is Gunung Jambangan deposits, Gunung Ajek-Ajek deposits, Gunung Kepolo deposits, Gunung Mahameru deposits, and Gunung Semeru deposits. The Gunung Jambangan deposits are the oldest, while the Gunung Semeru deposits are the youngest. These deposits consist of lahars, lava flows, pyroclastic fall deposits, pyroclastic flow deposits, and volcanic rock falls. The eruptions from

Mount Semeru generally have a basal andesite composition found in lava flows. The volcanic rocks on Mount Semeru mostly have a porphyritic hypocrystalline texture containing olivine, plagioclase, pyroxene, and opaque minerals. Examples of these volcanic rocks include andesite and basalts, with silica content ranging from 46.5% to 60% (Geologi, 2014; Hariyono and L., 2017).

2.2 The Eruption of Mount Semeru in 2021-2022

Mount Semeru has experienced several eruptions since 1818 up to the present day. It is considered one of the most active volcanoes in East Java. The volcano exhibits a Strombolian eruption type due to the fragmentation of low-viscosity basaltic magma. However, it is sometimes referred to as Vulcanian because it has produced lava domes, pyroclastic flows, basaltic lava, and pyroclastic clouds. Mount Semeru is also known for its frequent eruptions, which often result in daily lava flows (Hariyono and L., 2017).

Over the past two years, there have been recorded eruptions from Mount Semeru. In 2021, various volcanic activities were observed, including material falls, pyroclastic flows, ash plumes, ash clouds, and mudflows. The most recent and significant eruption occurred on December 4, 2021. During this event, a pyroclastic eruption cloud reached a height of 11 kilometers and traveled towards the Pronojiwo and Sumberwuluh districts in Lumajang, East Java. This eruption also triggered mudflows, explosive material ejections, and ashfall. Additionally, there were reports of eruption earthquakes, blast earthquakes, deep volcanic earthquakes, and distant tectonic earthquakes that damaged hundreds of buildings, houses, transportation networks, farmland, and resulted in casualties (Prasetiawan, 2021). As of March 27, 2022, Mount Semeru continued to exhibit activity with an ash column reaching 4,676 meters above sea level, recorded by seismographs with a maximum amplitude of 20 mm and a duration of 294 seconds (Pura, 2022). Other ongoing activities included ash plumes, pyroclastic flows, and crater incandescence. These activities persisted until October 2022, with several appearances of volcanic ash plumes at varying heights. (Global Volcanism Program, 2022).

2.3 Volcanic Eruptions

The volcanic activity of Mount Semeru has shown continuous eruptions since 1818 until today. An eruption itself is defined as the eruption of a volcano or the release of oil and hot vapor sources (KBBI, 2016). Eruptions can occur due to the unstable conditions of the magma chamber inside the volcano, causing magma to exit through openings to the Earth's surface. Magma that exits to the surface is referred to as lava (USGS, 2022). Not only magma, but the instability of the magma chamber can also push other materials to exit as a result of the accumulation of eruptions in the days before (Aprillya, 2021).

The process of magma exiting the volcano's chamber consists of effusive and explosive phases. Effusive is the process where magma slowly exits and becomes lava, forming a lava flow. On the other hand, explosive is the process where magma exits and causes explosions. This process is also influenced by the characteristics of the lava. If the lava is more fluid, gases will escape more easily.

However, if the lava is viscous, gases will have difficulty escaping. As a result, fluid lava will flow more quickly, while viscous lava will flow more slowly (USGS, 2022).

Based on the type of eruption strength, eruptions are classified into six types: Hawaiian, Strombolian, Plinian, Vulcanian, Surtseyan, and Phreatoplinian. The Hawaiian type falls under explosive eruptions with basaltic magma characterized by the emission of lava fountains and lava flows in rift zones. The Strombolian type is also characterized by the emission of lava fountains from volcanoes located at continental margins or within continents. The Plinian type is an explosive eruption with acidic magma and high viscosity, composed of andesite to rhyolite (Sub-Plinian). This type emits materials like pumice (Ultra-Plinian) in significant quantities. The Vulcanian type is an eruption type with andesitic to dacitic magma characterized by volcanic bombs and debris around the crater. The Surtseyan type is an eruption that involves the interaction between basaltic magma and surface or subsurface water, resulting in an eruption known as phreatomagmatic. Meanwhile, the Phreatoplinian type is an eruption that also involves the interaction between magma and water, which is typically rhyolitic. Therefore, both of these types often occur in underwater volcanoes or volcanic crater lakes (ESDM, 2023).

The types of eruptions based on their explosiveness are related to the cause of the eruption. There are terms like magmatic, phreatic, and phreatomagmatic eruptions. Magmatic eruptions are explosive, effusive, or mixed eruptions caused by magma breaking through the Earth's surface (MAGMA Indonesia, Erupsi

Magmatik, 2021). Phreatic eruptions, or steam explosions, occur when magma encounters groundwater or surface water. Due to the extreme temperature difference, water vaporizes, resulting in explosions characterized by steam, water, ash, rocks, and volcanic bombs (MAGMA Indonesia, Erupsi Freatik, 2021). Phreatomagmatic eruptions occur due to the interaction between phreatomagmatic or explosive magma and water (MAGMA Indonesia, Phreatomagmatic, 2021). These eruptions fall under the category of Surtseyan eruptions.

There are two causes of volcanic eruptions. The first cause is internal factors, which involve eruptions due to activities inside the volcano. These eruptions are related to magmatic eruptions. Eruptions caused by internal factors have been observed by Konstantinou et al. (2013), who analyzed tremor earthquakes at Mount Semeru from November 22 to December 31, 2009, to differentiate between explosive and effusive eruption records. Both types of eruptions resulted in the conclusion that magma was extruded to the Earth's surface through fissures/faults. This means that the eruptions in 2009 occurred due to internal factors.

The second cause is external factors, which involve eruptions triggered by events around the volcano, such as a collapse. A collapse occurs when a landslide occurs above the magma chamber. Landslides can be caused by external factors like heavy rainfall. When frequent rainfall occurs, a significant amount of water enters the cracks in the lava dome and reacts with the materials inside the volcano. Volcanic ash material that has dried up at the top of the mountain can also be eroded by rainwater. This condition causes the volcanic ash covering the mountain's summit to disappear, allowing the volcano to erupt its internal materials when there are openings for them to escape (Permana, 2021). The occurrence of a collapse as an external factor has been observed by Farquharson and Amelung (2020) at Kilauea Volcano, Hawaii, in May 2018. It was suggested that heavy rainfall could be a trigger for volcanic activity, and the collapse occurred at that volcano due to extremely heavy rainfall. Another study by Farquharson and Amelung (2022), which observed volcanic activity due to increased rainfall and global warming, also concluded that external factors can trigger volcanic activity, such as the rupture of a lava dome. Thus, external factors, not just internal factors, can contribute to volcanic activity in volcanoes.

2.4 Remote Sensing for Volcano Observation

Remote sensing is one of the methods used for observing volcanoes. Remote sensing is the science of acquiring information from Earth's surface without direct contact. This process involves capturing energy that is reflected or emitted from the Earth's surface using instruments such as balloons, aircraft, and satellites (Sutanto, 1994 as cited in Muhsoni, 2015). The data collected by these instruments are then processed, analyzed, and applied as needed (Lillesand, Kiefer, and Chipman, 2004 as cited in Muhsoni, 2015).

Remote sensing systems involve energy sources such as solar radiation, heat radiation, the atmosphere, and the Earth's surface interacting with energy sources, sensors that capture surface visualizations, data processing, and data utilization. This system can be seen in Figure 2.2.

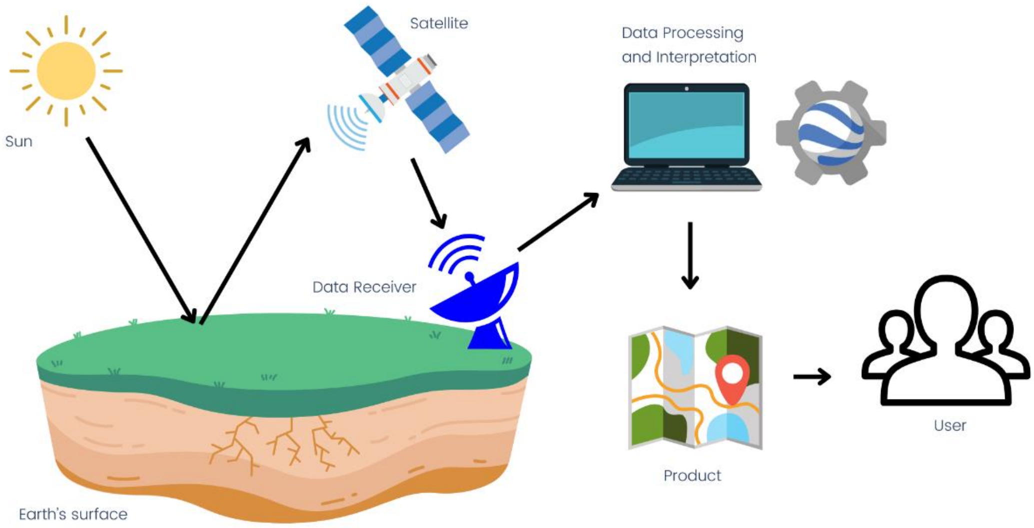

Figure 2.2 Remote Sensing Systems

Energy from the sun provides illumination to the Earth's surface, making it clear and visible to sensors. These sensors record and collect the information, which is then transmitted to stations for data processing. The processed data is stored in a server in a format that allows users to access it freely and easily (Lillesand, Kiefer, and Chipman, 2004, as cited in Muhsoni, 2015; Sanderson, 2006).

Remote sensing utilizes the spectrum of energy and electromagnetic wave radiation from an energy source. There are two types of remote sensing systems based on their energy source: active systems and passive systems. Active systems involve data collection with the use of pulsed energy, such as radar. On the other hand, passive systems gather data with the assistance of solar energy (Muhsoni, 2015).

There are various applications of remote sensing, especially in monitoring volcanic activities. Examples of using remote sensing methods for observing volcanic activity include thermal volcanic system monitoring in active Latin American volcanoes using ASTER and MODIS sensors (Reath, et al., 2018), the reconstruction of the 2014-2015 eruption of Mount Fogo using MODIS and SEVIRI thermal sensors (Miranda, et al., 2022), and the observation of the morphological evolution of Krakatau Volcano using SAR and optical remote sensing data (Xiang, et al., 2022).

In conducting volcano observations using remote sensing methods, an example of a satellite that can be used is Planet NICFI. The Planet NICFI satellite has a spatial resolution of 4.77 meters, and its data can be easily and freely accessed through the Google Earth Engine platform (Planet Team, 2017). This satellite is more commonly used for classifying and mapping deforestation land use (Wagner, et al., 2023; Masolele, et al., 2022). Due to its high spatial resolution, the results provided are capable of representing deforestation mapping very effectively (Wagner, et al., 2023). Therefore, it can provide excellent observations when applied to natural volcano image conditions, surpassing the spatial resolution of Sentinel-2 satellites, which typically range from 10 to 60 meters and are often used for volcano monitoring.

Another satellite that can be utilized is Landsat 8. Landsat 8 is a satellite launched in 2013 from Vandenberg Air Force Base, California. It has a spatial resolution of 30 meters, Operational Land Imager (OLI) instrument, and Thermal Infrared Sensor (TIRS) instrument. The OLI instrument consists of the near-infrared and shortwave infrared spectrums, while the TIRS instrument can measure land surface temperature (LST) (USGS, 2013). Landsat 8 is often used to observe thermal anomalies in the monitoring of ash plumes and volcanic activities around volcanoes (Blackett, 2014). It has also been used to assess temperature changes within the caldera of Mount Rinjani and has shown promising results, especially for predicting Strombolian eruptions (Suwarsono et al., 2016). Therefore, the TIRS instrument on Landsat 8 for detecting thermal anomalies can be employed to observe conditions at Mount Semeru.

The use of other data to support volcano observations includes CHIRPS. Climate Hazards Group InfraRed Precipitation with Station Data (CHIRPS) is a rainfall dataset available since 1981 by USGS and CHC. This data provides time-series satellite images of rainfall and seasonal drought monitoring. CHIRPS has a spatial resolution of 5,566 meters and a temporal resolution of 1 day (Earth Engine Data Catalog, 1981; CHC, 2022). CHIRPS has only one band, the precipitation band. An example of CHIRPS data usage is demonstrated by Hsu et al. (2021), which validated CHIRPS for rainfall estimation in Taiwan. Compared to IMERG data, CHIRPS can capture temporal variations in rainfall across various time scales for each day. Another study by Rahmawati, Rahayu, and Yuliasari (2021) also found that CHIRPS can detect light rain, heavy rain, and wet periods with good performance compared to TRMM data. The accuracy of CHIRPS in estimating rainfall amounts is also superior to GPM IMERG and TRMM. Therefore, CHIRPS can be applied for observing rainfall at Mount Semeru.

CHAPTER III

RESEARCH METHODOLOGY

The research workflow is divided into four stages: data preparation, data preprocessing, data processing, data comparison and correlation, and drawing conclusions. Specifically, this workflow can be seen in the flowchart illustrated in Figure 3.1.

In the data preparation stage, all the required images are collected from various satellite sources. For observing the morphology and wetness of Mount Semeru, Planet & NICFI Basemaps satellite imagery is used. Thermal observations are conducted using Landsat 8 satellite images, while rainfall observations utilize CHIRPS data. Each collected dataset goes through a preprocessing process to obtain the desired visualizations, including cloud filtering, time filtering, and location filtering. The next stage is data processing, which involves visualizing each filtered satellite image using various bands and colors. The output of each parameter also includes time series graphs that are useful for correlating parameter values and comparing their changes. Therefore, in order to draw conclusions regarding the causes of eruptions, a data comparison and correlation stage is necessary.

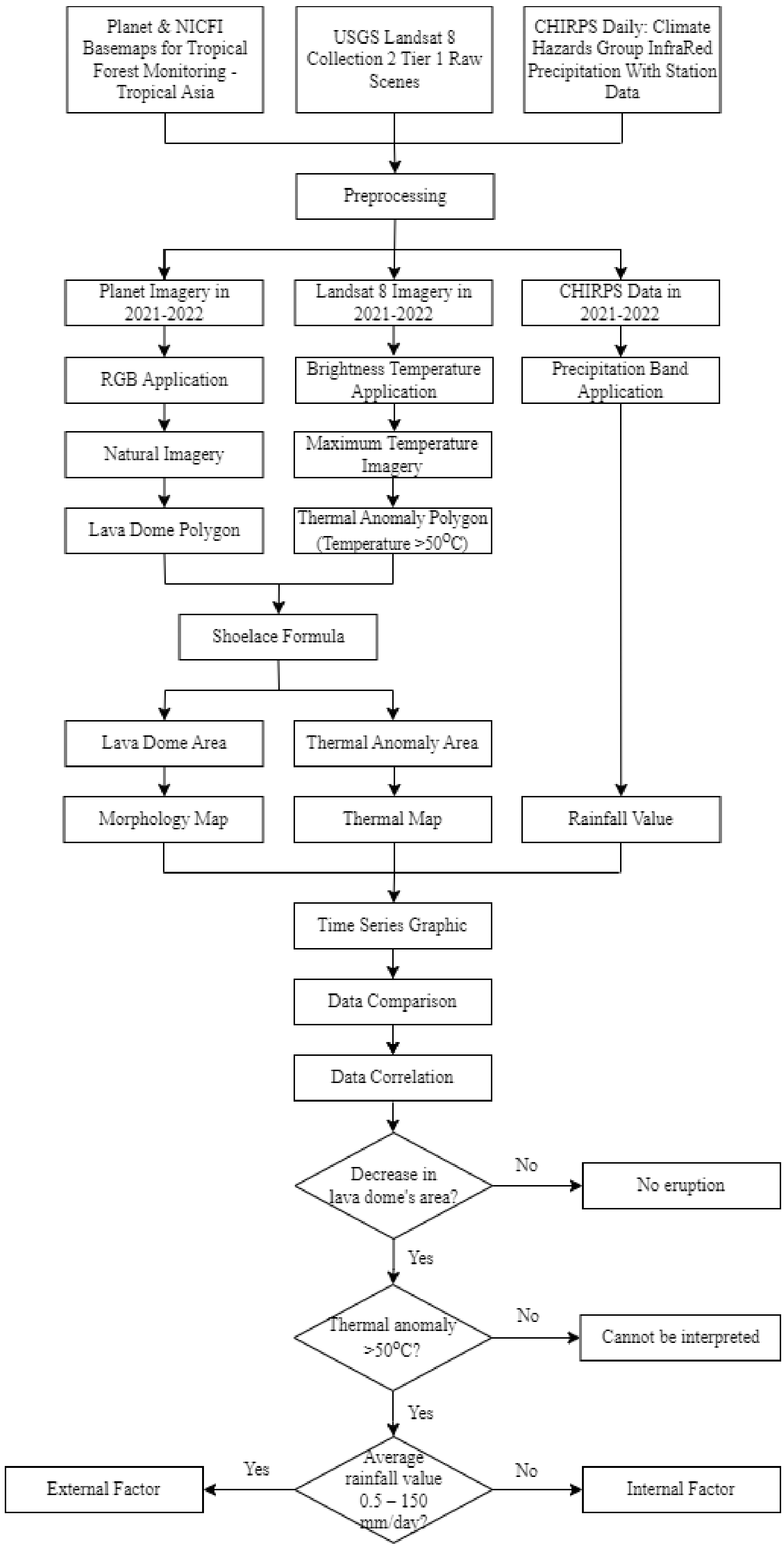

Figure 3.1 Research Workflow Diagram

All these stages are carried out using the Google Earth Engine (GEE) platform, which is a cloud computing platform launched by Google in 2010 (Kumar and Mutanga, 2019). GEE is one of the largest platforms for accessing satellite data in remote sensing applications. Users can access GEE through an internet-based Application Programming Interface (API). The data accessible through GEE is considered big data and can be accessed without the need for downloading it first (Amani, et al., 2020). GEE provides access to data from satellites like Planet NICFI, Landsat 8, and CHIRPS, which are available for free. The comprehensive bands available from each satellite are highly beneficial for visualizing the morphology, thermal, and rainfall data for Mount Semeru. Therefore, the use of GEE for monitoring Mount Semeru, considering its ease of access and data availability, is deemed suitable and can be utilized.

3.1 Data Preparation

Data preparation is carried out to obtain the desired visualization of satellite images. Firstly, data is collected from various types of satellites based on their spatial and temporal resolution, as well as their suitability for displaying the required data.

The observations are focused on Mount Semeru in terms of morphology, thermal, and rainfall. Therefore, the satellite images used to support the observation of morphology are from the Planet NICFI satellite, thermal observations are from the Landsat 8 satellite, and rainfall observations are based on CHIRPS data. In detail, all satellite images along with their resolutions and uses utilized in this research are presented in Table 3.1.

Table 3.1 Satellites Used in the Study (Earth Engine Data Catalog, 1981; 2013; 2015; Katalog Inderaja, 2018; The European Space Agency, 2023)

Satellites	Spatial Resolution	Temporal Resolution	Used
Planet & NICFI Basemaps for Tropical Forest Monitoring - Tropical Asia	4,77 meters	5,5 days	Observing the morphology using natural imagery on Mount Semeru in 2021-2022 to determine the area of the lava dome.
USGS Landsat 8 Collection 2 Tier 1 Raw Scenes	15-30 meters	16 days	Observing the thermal activity of Mount Semeru in 2021-2022 to determine the thermal anomalies area based on a specific threshold value.
CHIRPS Daily: Climate Hazards Group InfraRed Precipitation With Station Data	5566 meters	1 day	Observing the rainfall at Mount Semeru in 2021-2022.

3.2 Data Preprocessing

Preprocessing data is a stage to apply filters to satellite images in order to obtain the desired visualization. The filters applied include cloud filtering, time filtering, and location filtering. Cloud filtering is applied to Landsat 8 satellite imagery. This filter is used to remove cloud interference from the visualization of the images, allowing the satellite image data to be free from clouds. Landsat 8 satellite uses a cloud masking filter to eliminate clouds and can display the condition of Mount Semeru free from clouds. The application of the cloud-free filter on Landsat 8 is shown in Figure 3.2.

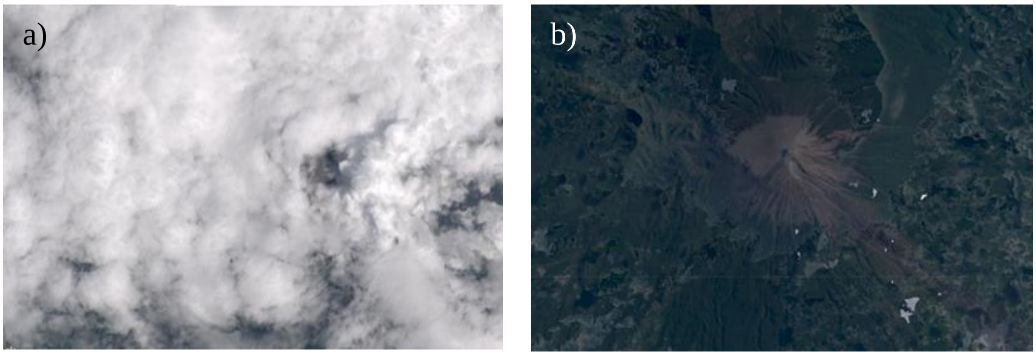

Figure 3.2 Cloud-Free Filter on Landsat-8 Satellite Imagery. a) Satellite image before cloud-free filtering, b) Satellite image after cloud-free filtering

The next filter is the location filter applied to all satellites. This filter serves to restrict the observation area to a single focus point, which is Mount Semeru. The application of this filter is done by creating a rectangle geometry on the Google Earth Engine platform. The geometry position is placed above Mount Semeru with a geometry size that can cover the entire area of Mount Semeru.

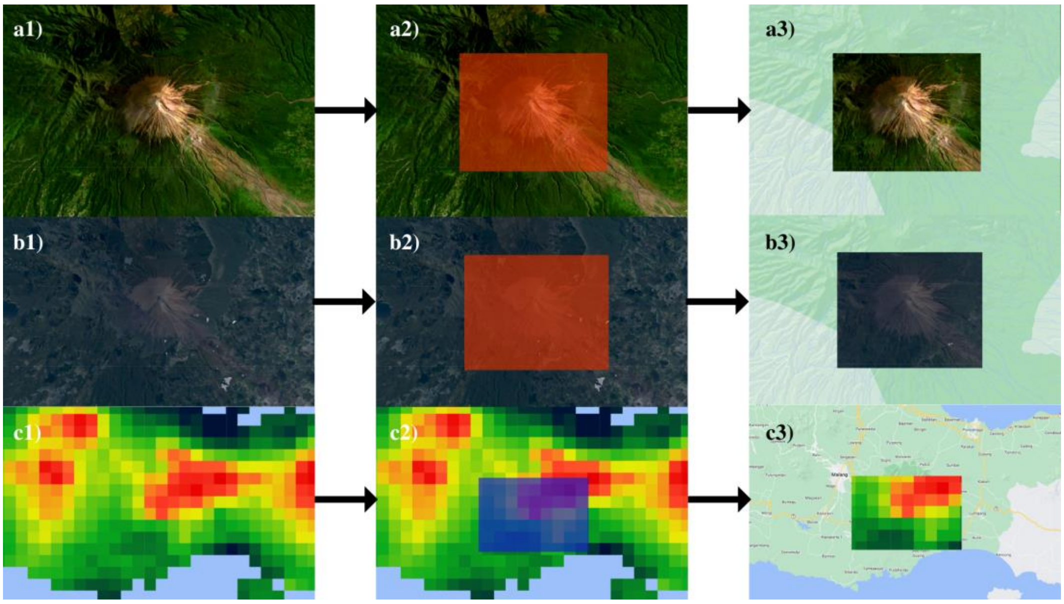

Figure 3.3 Location Filter on Satellite Images a) Planet NICFI, b) Landsat 8, c) CHIRPS

The final filter is the time filter applied to all satellites. This is because the observation of Mount Semeru only focuses on the year 2021-2022 from January to December to compare the conditions before and after the eruption. Therefore, each satellite will make observations every month from January 1st to December 31st.

3.3 Data Processing

The data processing stage is the stage of displaying visualizations from each satellite using various bands. These band variations can divide each image into displays that support morphology, thermal, and rainfall data. In general, the bands used for each satellite are presented in Table 3.2.

Table 3.2 The Bands Used on Each Satellite (Earth Engine Data Catalog, 1981; 2013; 2015; Katalog Inderaja, 2018; The European Space Agency, 2023)

Satellite	Used	Band
Planet & NICFI Basemaps for Tropical Forest Monitoring - Tropical Asia	Morphology	**Natural** B4: Red B3: Green B2: Blue
USGS Landsat 8 Collection 2 Tier 1 Raw Scenes	Thermal	**Thermal** B10: Brightness Temperature
CHIRPS Daily: Climate Hazards Group InfraRed Precipitation With Station Data	Rainfall	**precipitation**

3.3.1 Morphology

Data processing to obtain morphological information is carried out using visualizations from the Planet NICFI satellite. Visualization from this satellite will apply the RGB band, which stands for Red, Green, Blue to obtain a natural image using median calculations on all available images. The image with the median value will represent the value for one month. This natural image can also show the shape of Mount Semeru's lava dome, which will be observed every month in 2021-2022 to see any changes, especially before and after the eruption.

The change in the lava dome can be quantitatively assessed by calculating its area using the Shoelace formula algorithm applied in ArcGIS. Before calculating the area, the lava dome is marked by creating a polygon that represents the lava dome area. Then, the Shoelace formula method is applied to delineate the polygon area representing the lava dome. The Shoelace formula is a method or theorem for calculating the area of a polygon based on the coordinates of each vertex. This method can be applied to polygons with triangular, quadrilateral, or n-sided shapes (Lim and Lee, 2017). In this research, the polygon created to determine the lava dome is of n-sided shape, so the following Shoelace method equation is used.

$$A = \frac{1}{2} z \tag{3.1}$$

$$z = \begin{bmatrix} x_i & x_{n-1} & x_n & x_1 \\ y_i & y_{n-1} & y_n & y_1 \end{bmatrix} \tag{3.2}$$

$$z = (x_1 y_{n-1} + x_{n-1} y_n + x_n y_1) - (x_{n-1} y_1 + x_n y_{n-1} + x_1 y_n) \tag{3.3}$$

Parameter A represents the area to be calculated, z is the cross-product operation component, n is the number of angles, x is the longitude coordinate, and y is the latitude coordinate. After calculating the lava dome's area, the next step is to display the area for each month in the form of a graph. The graph will show the data's characteristics in terms of the significant changes in area that occur each month before and after the eruption.

The determination of the lava dome boundary for area calculation is based on two factors. The first factor is based on the characteristics of the lava dome itself. Lava domes are formed by the eruption of viscous magma, which accumulates in a vent (Tienrey, 2010). Lava domes typically have steep sides and rough surfaces (NPS, 2023). The location of the lava dome formation is often in the center of the crater or far from the crater (Britannica, 2016). Based on these characteristics, the part of the lava dome located in the center of Mount Semeru's crater is marked, as shown in Figure 3.4.

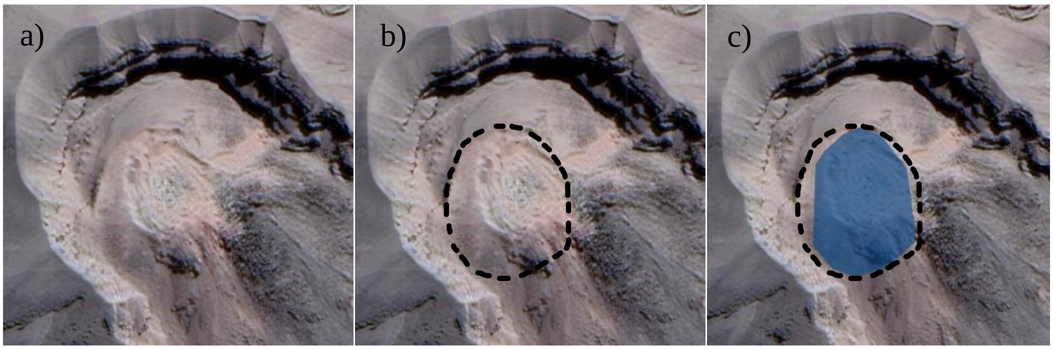

Figure 3.4 Lava Dome from Google Earth Satellite Image (Last Updated in 2023). a) Image of Mount Semeru's Lava Dome, b) Image of Mount Semeru's Lava Dome Along with the Lava Dome Boundaries Based on Its Characteristics, c) Image of Mount Semeru's Lava Dome Along with the Lava Dome Boundaries and the Location of Thermal Anomalies at the Summit

The second factor is the alignment of the location where thermal anomalies are detected with the shape of the lava dome. In the results of the morphology and thermal imagery, when overlaid as shown in Figure 3.4, it can be observed that the majority of the thermal anomalies are located within the defined polygon area of Mount Semeru's lava dome. This indicates that the detected thermal anomalies can serve as one of the indicators of the location of Mount Semeru's lava dome.

3.3.2 Thermal

The data processing to obtain thermal information is carried out using Landsat 8 satellite imagery. Visualization from this satellite will be applied using the Brightness Temperature band, calculated using the maximum value for each available image. The result is a visualization of the maximum temperature imagery on Mount Semeru, which can indicate thermal anomalies. Thermal anomalies are determined based on a temperature threshold. In this case, a threshold of 50℃ is used, as determined by the research conducted by Aufaristama, et al. (2018), who used this value as a threshold. This is because a temperature of 50℃ is the lowest temperature at which volcanic activity occurs at an Icelandic volcano. Therefore, this value will be applied to Indonesian volcanoes, including Mount Semeru. It is expected that this value will also be able to detect the small eruptions that occur at Mount Semeru almost daily (Hariyono and L., 2017). Based on these conditions, pixels with values above 50℃ will be considered as thermal anomalies, indicating volcanic activity at Mount Semeru. Thermal anomaly observations are conducted only for the months that detect the presence of thermal anomalies in the 2021-2022 timeframe.

After obtaining thermal anomalies for specific months, the next step is to calculate the area of thermal anomalies using the shoelace formula method. The thermal anomalies, represented as polygons, are calculated for their area using equation (3.1). The values for the area of thermal anomalies for each month will be presented in the form of graphs to observe the significant changes in area before and after the eruption.

3.3.3 Rainfall

Processing rainfall data using CHIRPS involves adding the 'precipitation' band after the preprocessing stage. The 'precipitation' band will display daily rainfall data, observed over two years from 2021 to 2022. After obtaining the rainfall images, the next step is to create a time series graph showing changes in rainfall throughout the year 2021-2022 to observe increases or decreases in rainfall at Gunung Semeru. The data displayed in the graph represents the monthly average values.

From these average values, the results will be matched with the threshold values of rainfall intensity classified by Badan Meteorologi, Klimatologi, dan Geofisika (BMKG) (2022) in Table 3.3.

Table 3.3 Rain Intensity Classification (BMKG, 2022)

Rainfall Value	Description
0 mm/day	Cloudy
0.5 – 20 mm/day	Light rain
20 – 50 mm/day	Moderate rain
50 – 100 mm/day	Heavy rain
100 – 150 mm/day	Very heavy rain
>150 mm/day	Extreme rain

3.4 Data Comparison and Correlation

The next step is to compare the data of each parameter to observe changes in their values, whether they increase or decrease. The comparisons made include the comparison of morphology data with thermal data, as well as the comparison of thermal data with rainfall data. After these three datasets are compared to observe their characteristics, the next step is to perform correlations on specific parameters.

The data correlation stage is the stage where relationships between each parameter are explored, allowing each dataset to be linked and analyzed more deeply. One of the simple analyses that can be used is a regression analysis. Regression analysis is an analysis of the relationship between two variables: the dependent variable (which depends on other variables) and the independent variable (which does not depend on other variables) (Seltman, 2018). If there is only one independent variable, this regression analysis is referred to as simple linear regression analysis. However, if there are more than one independent variables, it is called multiple linear regression analysis. In this study, simple linear regression analysis will be used to examine the correlation between morphology and thermal parameters, morphology and rainfall, and thermal and rainfall. Simple linear regression analysis utilizes the relationship between the independent variable (X) and the dependent variable (Y) based on the following equation (Yuliara, 2016; Seltman, 2018).

$$Y = a + bX \tag{3.4}$$

Parameter Y represents the regression line as the dependent variable, a as the constant (intercept), b as the constant (slope), and X as the independent variable. To find the values of a and b, the following equation is used (Yuliara, 2016).

$$a = \frac{(\Sigma Y_i)(\Sigma {X_i}^2) - (\Sigma X_i)(\Sigma X_i Y_i)}{n\Sigma {X_i}^2 - (\Sigma X_i)^2} \tag{3.5}$$

$$b = \frac{n(\Sigma X_i Y_i) - (\Sigma X_i)(\Sigma Y_i)}{n\Sigma {X_i}^2 - (\Sigma X_i)^2} \tag{3.6}$$

The variable n represents the number of data points.

Examining a correlation in data can be done by creating a scatter plot. A scatter plot can show several forms of correlation. The first type is positive correlation, where when X has a high value, Y also has a high value, and vice versa (a direct relationship). The second type is negative correlation, where when X has a high value, Y has a low value, and vice versa (an inverse relationship). The last type is no correlation, where the value of X tid cannot explain or predict the value of Y, and vice versa (Gerstman, 2016).

In regression analysis, there is a coefficient that can indicate the strength of the relationship between variables X and Y, which is the correlation coefficient (Yuliara, 2016). The formula for the correlation coefficient (r) is as follows.

$$r = \frac{n\Sigma X_i Y_i - (\Sigma X_i)(\Sigma Y_i)}{\sqrt{(n\Sigma X_i{}^2 - (\Sigma X_i)^2)(n\Sigma Y_i{}^2 - (\Sigma Y_i)^2)}} \tag{3.7}$$

The larger the value of the correlation coefficient (approaching 1 or 100%), the stronger the relationship between variables X and Y. Conversely, the relationship is considered weak to non-existent when the correlation coefficient approaches zero or is equal to zero. The classification of correlation coefficient values along with their descriptions is presented in Table 3.4.

In addition to the correlation coefficient, there is a term called the coefficient of determination, which is the square of the correlation coefficient (r^2). The squared result of the correlation coefficient indicates the extent to which variable X can explain variable Y, while the difference between the total value (1 or 100%) and the coefficient of determination indicates the extent to which variable Y can only be explained by variables other than X (Yuliara, 2016).

Table 3.4 Classification of Criteria for Correlation Coefficient Values (Sugiyono, 2019 in Araffah and Purnama, 2020)

Interval Coefficient	**Description of Relationship**
0,00 - 0,199	Very Low
0,20 - 0,399	Low
0,40 - 0,599	Moderate
0,60 - 0,799	Strong
0,80 - 1,000	Very Strong

In this research, correlations between morphology and thermal, as well as between thermal and rainfall, will be investigated. The area of the lava dome in the morphology parameter will be used in the data correlation. One value of the lava dome area will represent one month. Similarly, the thermal parameter will use the area of thermal anomalies in the data correlation, and one value will represent one month. As for the rainfall parameter, the average value for each month will be considered, so one value will also represent one month. Therefore, the correlations between the three parameters will be assessed based on their monthly values.

After comparing and correlating the data, the next step is to determine the cause of the eruption. Based on the workflow and results, it can be concluded whether the eruption of Mount Semeru in December 2021 was due to internal (magmatic) factors that led to increased volcanic activity or external factors (rainfall) that caused a collapse in the mountain's dome. The determination of these two factors is based on the criteria presented in Table 3.5.

The morphology, specifically the observation of lava domes, will always undergo changes when an eruption occurs. When searching for the area of the lava dome, a significant decrease in area will be found before, during, and after the eruption. Therefore, changes in morphology will always occur, especially in terms of the reduction in the lava dome area.

Thermal observations with the measurement of anomaly areas using a threshold above 50℃ can indicate an increase in volcanic activity that is approaching the summit of the mountain or has reached the surface. Thermal anomalies below the 50℃ threshold are less likely to represent the temperature when an eruption occurs. Therefore, the threshold condition above 50℃ can be an indicator of the reason for the eruption of Mount Semeru.

The primary determinant among the three parameters is rainfall. There is a difference in rainfall values to indicate whether the eruption of Mount Semeru occurred due to internal or external factors. If the rainfall value is 0 mm/day (cloudy), it means that there is no rain factor that can moisten and affect the conditions on Mount Semeru. Conversely, if the rainfall value is above 0 mm/day (light rain to extreme rain), there is a possibility that it triggered the eruption of Mount Semeru.

Table 3.5 The Parameter Causing Mount Semeru's Eruption in December 2021

Morphology	**Thermal**	**Rainfall**	**Causes**
Decrease in the lava dome area	Thermal anomaly >50℃	Average rainfall of 0 mm/day in several months before the eruption	Internal Factor
Decrease in the lava dome area	Thermal anomaly >50℃	Average rainfall >0 mm/day in several months before the eruption	External Factor

CHAPTER IV

RESULTS AND DISCUSSION

Results and discussion consist of several sections. The first section includes visual analysis and graphs for the parameters of morphology, thermal, and rainfall. The second section involves comparing and correlating each dataset to understand the relationships between the parameters. The third section is the discussion, where conclusions are drawn based on the results of the three parameters, and any limitations of the research are discussed.

4.1 Morphology

Morphological analysis was conducted using Planet NICFI satellite data with observations spanning from January 2021 to December 2022. Observations were carried out every month with a total of 16 data points out of 24. Eight data points were not used due to poor data quality caused by cloud cover. The visual representation of the lava dome's morphology for several months in 2021 is presented in Figure 4.1.

In general, the morphology of the lava dome from January to October 2021 did not show significant changes. This is evidenced by the lava dome's area calculated using the shoelace formula method. This method was applied to the lava dome's polygon using equation (3.1) and is illustrated in Figure 4.2. Throughout the months from January to October 2021, the area of the lava dome remained in the range of 18,000 to 27,000 m^2. Although there were fluctuations in the lava dome's shape, especially in August to September 2021, which experienced a 34% decrease in area compared to August, the overall lava dome area remained within the same range from January to October 2021. Despite the detected eruptions, such as material falls, pyroclastic flows, ash clouds, lahars, and ash plumes during this period, they did not affect the lava dome's area.

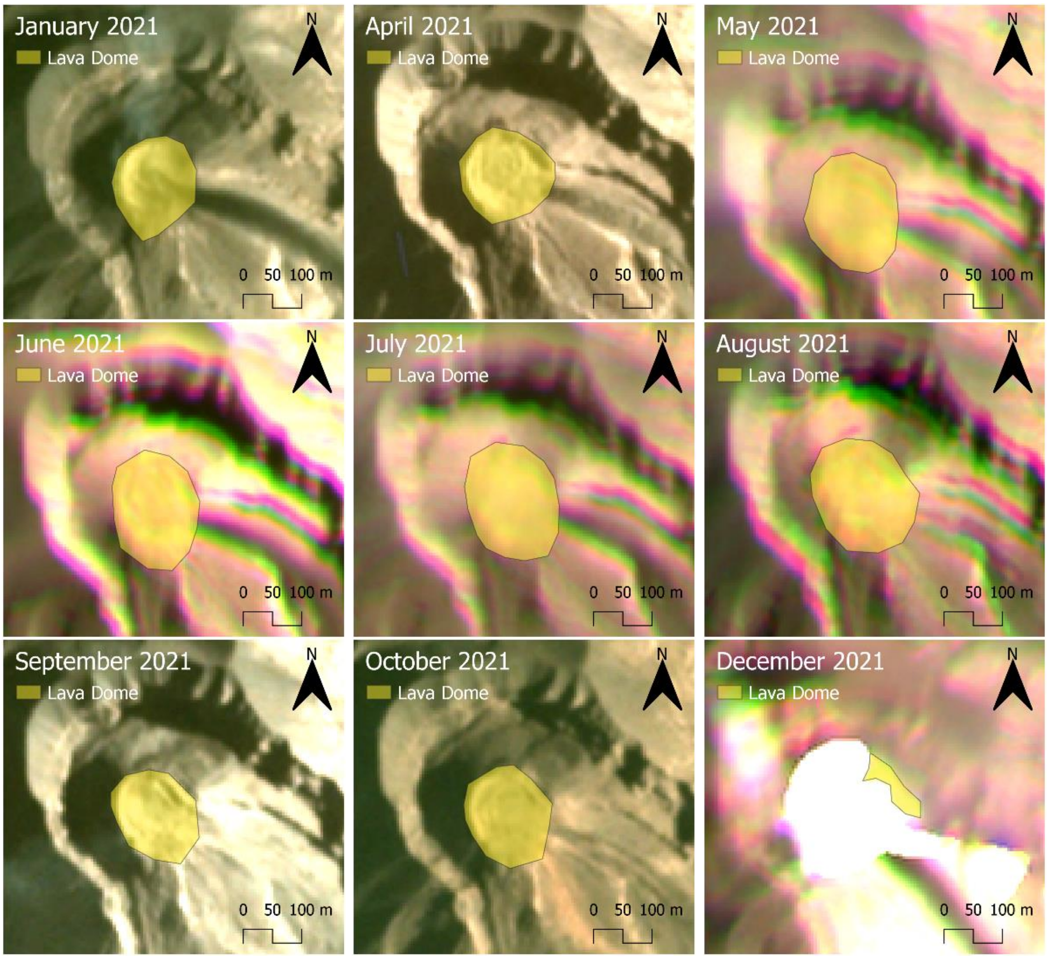

Figure 4.1 Lava Dome (Highlighted by Polygon) on Planet NICFI Natural Satellite Image in 2021

The significant change in the lava dome's shape occurred from October to December 2021, with a reduction in area of 16,138 m^2 or 81% of the lava dome's area in October, as shown in Figure 4.2. Compared to the decreases in August and September, the events in October and December represent a more substantial reduction. The lava dome's area in December 2021 is related to the eruption of Mount Semeru. According to the Global Volcanism Program's report (2022), the Jonggring Seloko lava dome at Mount Semeru collapsed from December 1-6, 2021, causing pyroclastic flows to move southeastward. These pyroclastic flows generated ash clouds reaching 50,000 feet above sea level. This activity continued throughout December 2021.

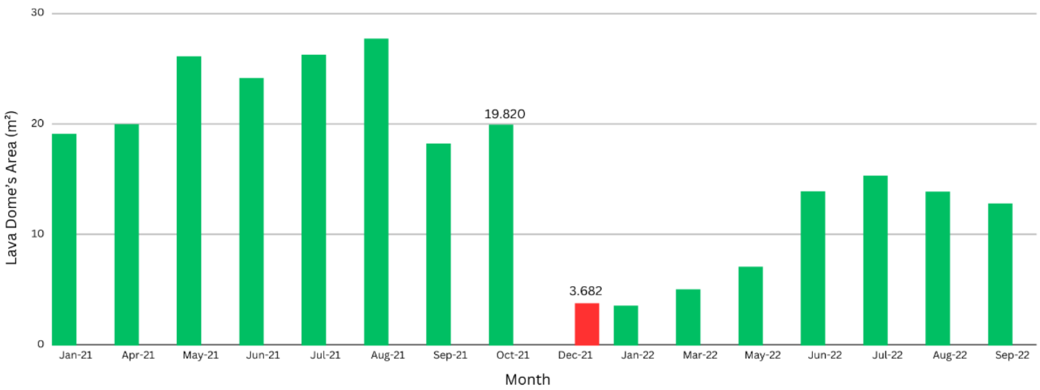

Figure 4.2 The lava dome area of Mount Semeru in 2021-2022. The red-colored portion represents December 2021, which is the month when the eruption occurred

Observations were also carried out throughout the year 2022 with the aim of assessing the conditions after the eruption in December 2021. The lava dome in 2022 can be seen in Figure 4.3.

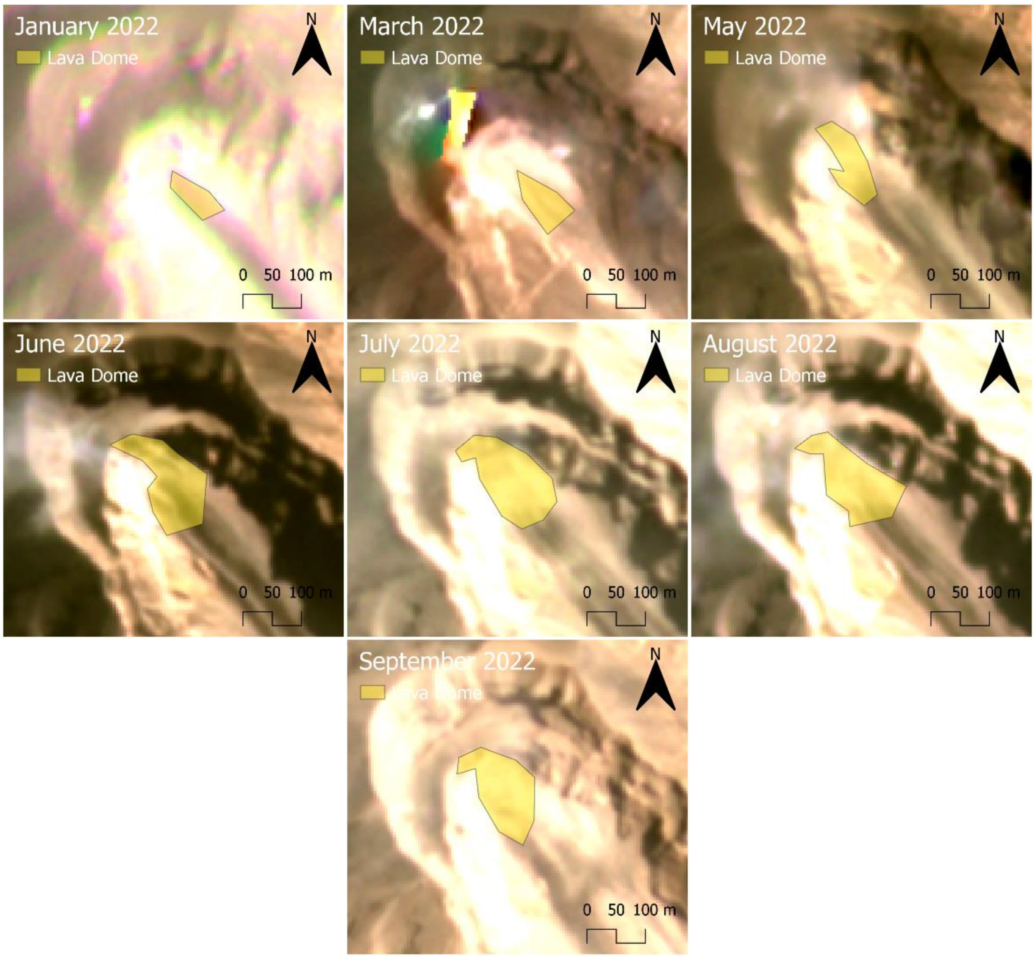

Figure 4.3 Lava Dome (Marked with a Polygon) on Natural Satellite Image from Planet NICFI in 2022

In January and March 2022, it can be observed that the lava dome did not undergo significant changes in size compared to December 2021. Referring to Figure 4.2, December 2021, January 2022, and March 2022 were within the range of 3,000-5,000 m^2 in size, followed by an increase in the lava dome's size in May 2022 by 29%. A relatively significant increase in size occurred in the months of May and June 2022, amounting to 49% of the June lava dome's size. After this increase in size, from June to September 2022, the size remained in a similar range, approximately 12,000-15,000 m^2. The addition of size over time is believed to be due to the lava dome starting to rebuild and reform after it was lost and shattered during the eruption in December 2021. Although the lava dome began to reform, there were still some volcanic activities occurring after the eruption. These activities continued from January to September 2022, such as pyroclastic flows, ash clouds, and ash plumes.

4.2 Thermal

The thermal analysis was conducted using Landsat 8 satellite data with observations spanning from January 2021 to December 2022, using maximum temperature values. Observations were made every month, amounting to 12 data points out of 24 available. There were 12 data points that were not used because thermal anomalies were not detected above the 50ºC threshold. The visualization of detected thermal anomalies for various months in 2021 is presented in Figure 4.4.

Based on Figure 4.4, there were six months with detected thermal anomalies throughout the year 2021: April, May, July, September, November, and December. The area of each thermal anomaly was calculated using the shoelace formula method in equation (3.1). Thermal anomalies detected in April, July, and November 2021 were located right at the peak or lava dome of Mount Semeru. According to Figure 4.5, the area of these anomalies ranged from 1,700 to 9,000 m^2. This indicates that high temperatures above 50ºC were located at the mountain's summit. On the other hand, thermal anomalies detected in May and September 2021, with temperatures above 50ºC, were detected both at the summit and outside the summit, covering an area of 12,500 to 22,000 m^2. The most significant difference observed was in the thermal anomalies detected in December 2021. Many thermal anomalies were detected compared to the previous months, covering an area of 106,166 m^2. This large area indicates very high temperatures at several points on the mountain in December 2021, likely due to the eruption.

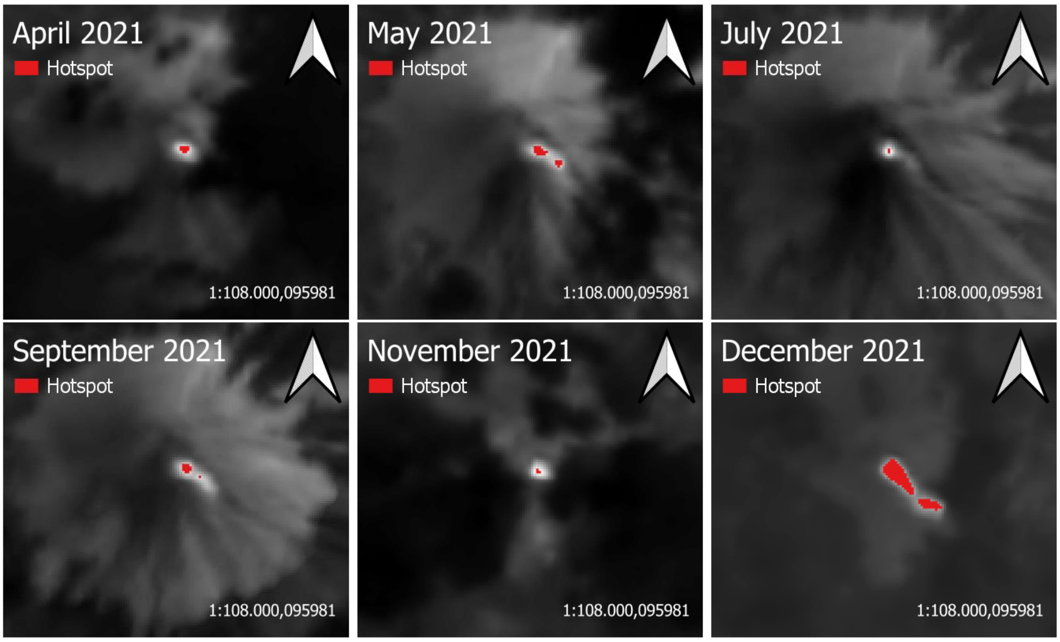

Figure 4.4 Thermal Anomalies (Marked with a Polygon) on Natural Satellite Image from Landsat 8 in 2021

The thermal anomalies detected on the summit and slopes of the mountain can occur due to volcanic activity near the detected location, either activity inside the volcano or already erupted at the surface. In April 2021, volcanic activity in the form of ash plumes occurred, while in May 2021, there were ash plumes and material fall activities. Material fall caused anomalies on the mountain's slopes in May 2022. Ash plumes alone were also detected in July, September, and November

2021. In December 2021, as the peak of the eruption, there were pyroclastic flows and ash clouds. These pyroclastic flows were responsible for the presence of thermal anomalies on the mountain's slopes during the eruption in December 2021.

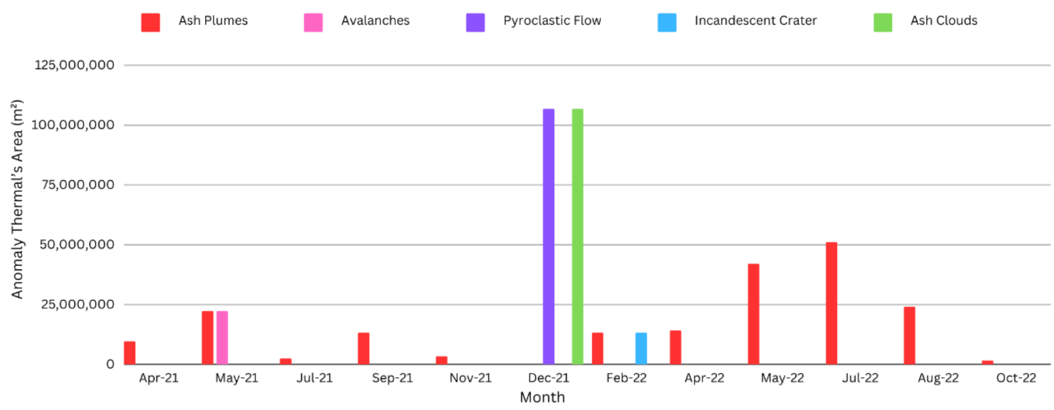

Figure 4.5 Area of Thermal Anomalies on Mount Semeru in 2021-2022. Data is accompanied by recorded volcanic activity information for each month

After observing the events before and during the eruption, observations were also made in several months in 2022 to see the conditions after the eruption. The results of the observations in 2022 are shown in Figure 4.6.

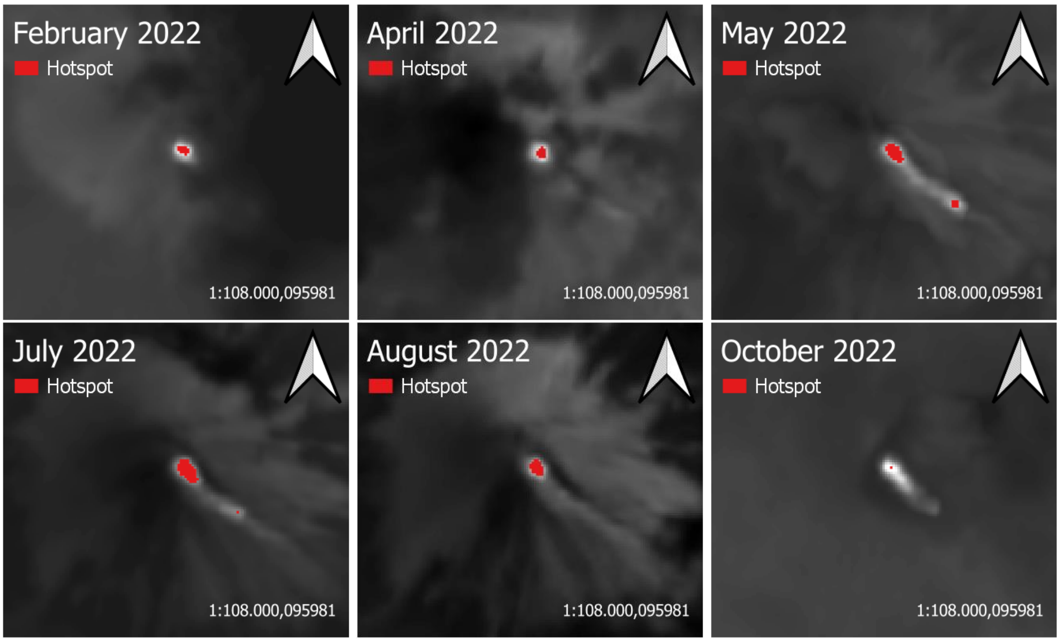

Figure 4.6 Thermal Anomalies (Marked with Polygons) on Landsat 8 Satellite Natural Images in 2022

In the period following the eruption, thermal anomalies were detected in six months, namely in February, April, May, July, August, and October 2022. Referring to Figure 4.5, the detected thermal anomalies tend to be more numerous compared to those in 2021, especially in February, April, July, August, and October 2022, showing thermal anomalies with areas ranging from 890 to 50,400 m^2 at the mountain's summit. Meanwhile, in May 2022, thermal anomalies were detected at the summit and on the mountain's slopes, covering an area of 41,386 m^2.

The thermal anomalies detected in several months in 2022 indicate that there were still eruptions occurring after the largest eruption in December 2021. In February 2022, there were activities like ash plumes and crater glow, while in April, August, and October 2022, only volcanic activities in the form of ash plumes were detected. In May and July 2022, there were ash plume activities that extended from the summit down to the mountain's slopes (Global Volcanism Program, 2022).

4.3 Rainfall

Rainfall data analysis was conducted using CHIRPS data with observations from January 2021 to December 2022. Rainfall observations were made every day in the area of Mount Semeru and its surroundings. This was done because CHIRPS data has a low spatial resolution of 5,566 meters, so a larger area was needed to analyze the rainfall conditions at Mount Semeru without pixelation. The detected daily rainfall values were averaged to represent the monthly values. The time series of rainfall values is presented in Figure 4.7.

The rainfall values during those two years exhibited significant fluctuations. The distribution of these values is also related to the occurrence of the rainy and dry seasons. The peak of the rainy season was in January and February, with a range of values from 14.8 to 19 mm/day for the year 2021, and 9 mm/day for the year 2022, as shown in Figure 4.7 (Ridwan, 2020). According to Table 3.3, rainfall values in the range of 0.5-20 mm/day still fall under the category of light rain. After that, there was a decrease in rainfall values in March and April 2021, indicating a reduction in rainfall intensity during those two months.

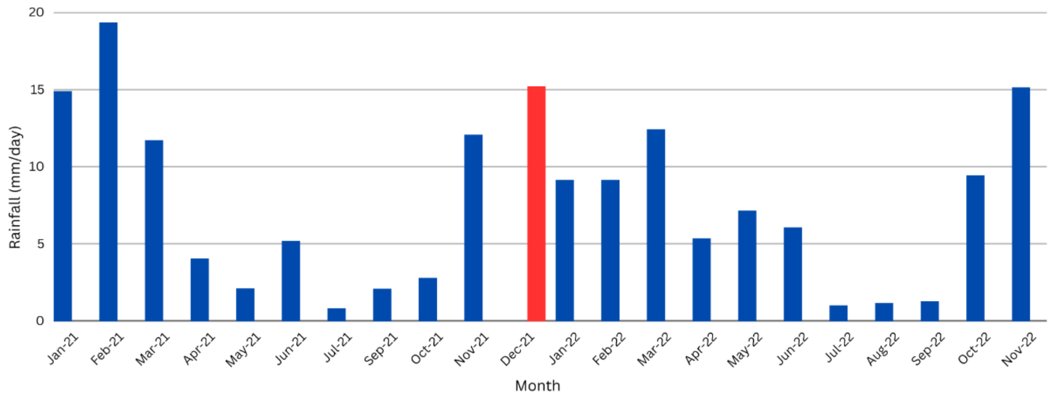

Figure 4.7 Rainfall Values of Mount Semeru for the Year 2021-2022. The month of December 2021 (highlighted in red in the graph) is the month of the eruption

Unlike in 2022, which experienced an initial increase in rainfall values in March 2022 followed by a decrease in April 2022, the values of rainfall in March and April 2021-2022 were in the same range, which was 3.9 - 12.3 mm/day. The onset of the dry season occurred in May and June 2021-2022, while the peak of the dry season happened in August 2021-2022 (Prasetyaningtyas, 2021; Warsudi, 2022). This is evident from the rainfall values in May and June 2021-2022, which were only in the range of 0-7 mm/day. In August 2021, there was no rainfall at all, classified as cloudy weather. However, August 2022 was classified as light rain with a rainfall value of 1 mm/day. In September, October, and November 2021-2022, there was an increase in rainfall values classified as light rain. A significant change occurred from October to November 2021, with a 77% increase because these months marked the beginning of the rainy season in 2021 (Prasetyaningtyas, 2021). However, the significant increase in rainfall values in 2022 happened from September to October 2022, with an 87% increase. This was due to September being the start of the rainy season in 2022 (Prasetyaningtyas, 2022). Rainfall values increased again in December 2021 by 20% compared to November 2021. December, which was the peak of the eruption of Mount Semeru (highlighted in red), also had relatively high rainfall compared to other months, with a value of 15.12 mm/day.

4.4 Data Comparison and Correlation

The results of the comparison between the lava dome's area in morphology, the area of thermal anomalies, and the rainfall values were analyzed to understand the characteristics of each dataset. The comparisons and correlations conducted were between morphology and thermal data, as well as between thermal and rainfall data. A comparison between the morphology's area (lava dome) and the area of thermal anomalies is illustrated in Figure 4.8.

Based on Figure 4.8, from January to October 2021 (before the eruption), the morphology area and thermal anomaly area had contrasting values. When the morphology had a large area of lava dome, the thermal anomaly had a small area. The events before the eruption in December 2021 showed that when the lava dome was still intact, there were not many detected thermal anomalies around the lava dome. Only a small area had temperatures above 50ºC. When we enter December 2021 as the month of the eruption, there was a change in the conditions, namely a drastic decrease in morphology area and a significant increase in thermal anomaly area. The relationship between these two parameters was still contrasting, but their values changed dramatically. This indicates that during the eruption, the lava dome broke and disintegrated, so the lava dome's area was no longer detected as before. However, the thermal anomaly area increased, and many areas were detected with temperatures above 50ºC.

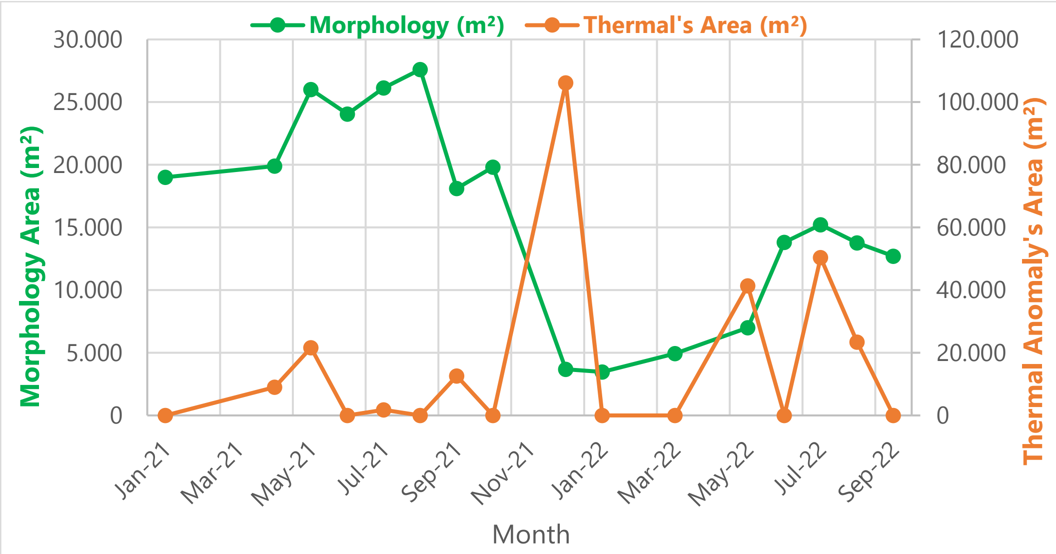

Figure 4.8 Comparison of Morphology Area with Thermal Anomaly Area in 2021-2022

In the post-eruption conditions (January-September 2022) in Figure 4.8, the relationship between morphology area and thermal anomaly area is not very clear because as the months progress, the morphology area increased while the thermal anomaly area fluctuated. During the period when the lava dome started to reform over the months, it seems that the thermal anomalies had varying areas, sometimes increasing and decreasing. The conditions before and after the eruption are confirmed by data correlation using simple linear regression analysis with the help of equations (3.4) and (3.7) shown in Figure 4.9.

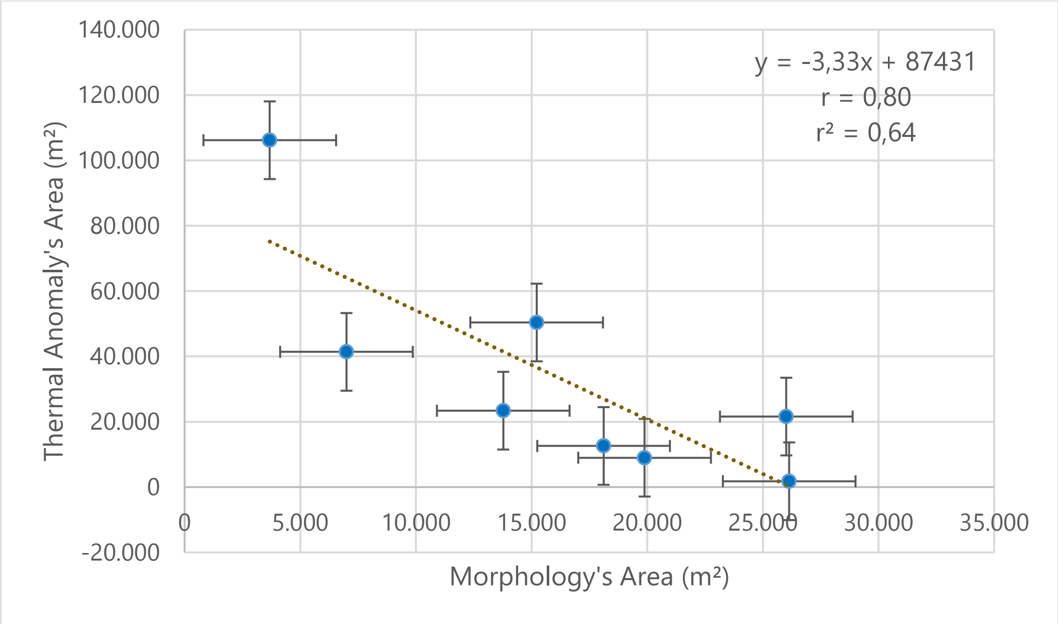

Figure 4.9 Correlation Between Morphology Area and Thermal Anomaly Area for 2021-2022

The correlation between the morphology area and thermal anomaly area for the year 2021-2022 in Figure 4.9 shows a negative correlation. This is evidenced by the negative values of *y* and the decreasing trendline. The correlation results align with the comparison in Figure 4.8, indicating that when the morphology area has a high value, the thermal anomaly area has a low value, and vice versa. Both parameters also exhibit a very strong correlation coefficient (*r*) based on Table 3.4. Since the correlation coefficient is 0.80 and falls within the interval of 0.8 to 1, this value is categorized as a very strong relationship. The morphology area value is capable of explaining and relating to the thermal anomaly area value, accounting for 64% based on the coefficient of determination (r^2) of 0.64.

After observing the comparison and correlation between the morphology area and thermal anomaly area, the next step is to compare the thermal anomaly area with rainfall, as shown in Figure 4.10.

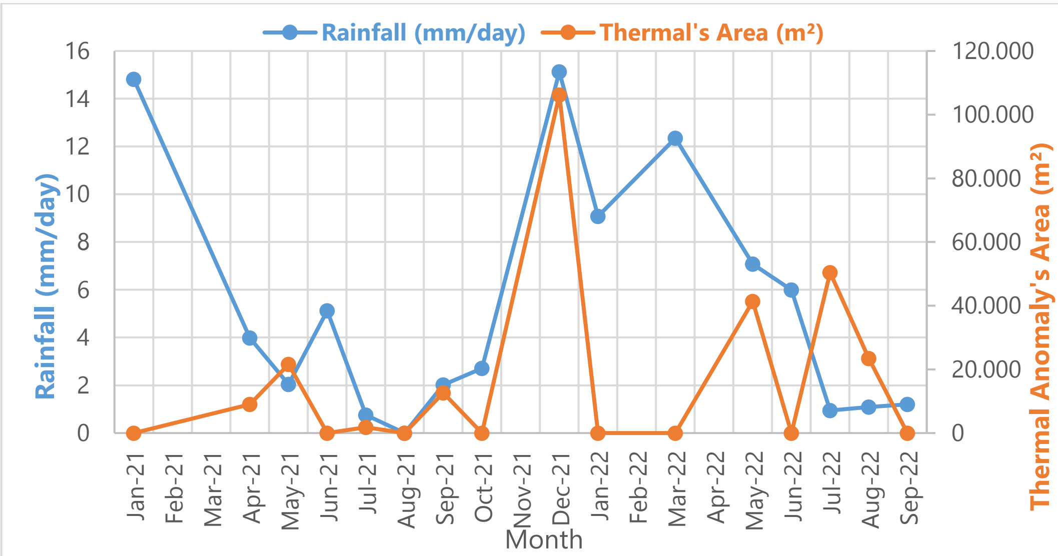

Figure 4.10 Comparison of Thermal Anomaly Area with Rainfall in 2021-2022

The comparison of the area of thermal anomalies and rainfall has varying relationships. Before the eruption occurred, there were several conditions where the area of thermal anomalies was low, but rainfall was high, as observed in January, April, June, and October 2021. Another condition was when the lines of the two parameters were nearly intersecting, as seen in May, July, August, and September 2021. The observation in December 2021, as the month of the eruption, showed a different relationship between thermal anomalies and rainfall, which was linear, meaning they both had high values.

The observations after the eruption from January to September 2022 showed predominantly high rainfall, but the area of thermal anomalies was relatively low, as seen in January to June 2022 and September 2022. However, in May 2022, there was still a correlation between rainfall and the area of thermal anomalies, although the values were not too far apart. In contrast, July and August 2022 witnessed a change in conditions, with a high area of thermal anomalies but low rainfall. When correlating the data, the resulting relationship is illustrated in Figure 4.11.

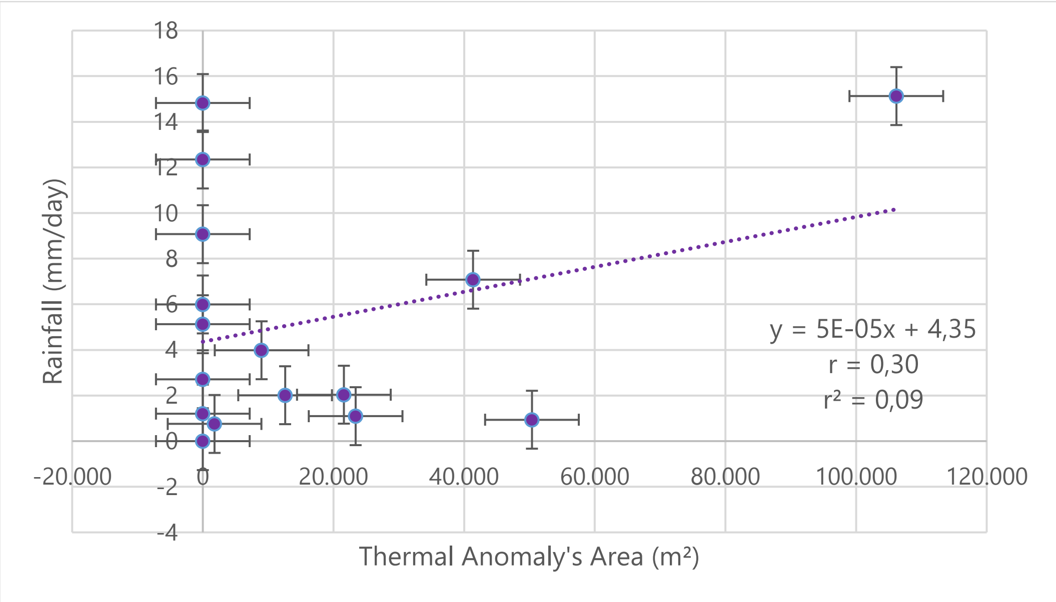

Figure 4.11 The Correlation Between Thermal Anomaly Area and Rainfall in 2021-2022

Based on Figure 4.12, the thermal anomaly area and rainfall have a positive but low correlation. This is related to Table 3.4, where the coefficient of correlation is 0.30, indicating a low level of correlation. When related to the coefficient of determination of 0.09, it means that there is only a 9% relationship between the thermal anomaly area and rainfall. In other words, the correlation between the thermal anomaly and rainfall parameters is not strong.

4.5 Discussion

The parameters of morphology, thermal, and rainfall yield results that can be summarized and related to the factors causing the eruption of Mount Semeru in Table 3.5. Morphological observations, especially the area of the lava dome, showed significant changes from October to December 2021. Based on the visualizations in Figures 4.1 and 4.3, the natural imagery in December 2021 appeared very bright, especially in the lava dome area. The difference between the polygons in October and December 2021 also indicates a significant change in the lava dome's condition, with a decrease in area of 16,138 m^2 or 81% as shown in the graph in Figure 4.2. This suggests that the lava dome indeed underwent changes in the form of a significant decrease in its area.

In the thermal observations, especially in terms of the area of thermal anomalies, there were several months with thermal anomalies detected with temperatures above 50ºC. These months include April, May, July, September, November, and December 2021, as seen in Figure 4.4, and February, April, May, July, August, and October 2022, as shown in Figure 4.6. All the detected thermal anomalies in these months had varying areas. There were volcanic activities within the mountain's interior, close to the surface, and they were detected to have temperatures above 50ºC. According to the graph in Figure 4.5, the thermal anomaly area in December 2021 was the largest among all the months, measuring

106,166 m^2. These anomalies were not only detected at the summit but also on the mountain's slopes, indicating that volcanic activity was not confined to the mountain's interior but had also reached the surface and the mountain's slopes. This signifies that an eruption did indeed occur in December 2021, with thermal anomalies detected at temperatures exceeding 50ºC.

In the rainfall observations, the distribution of values corresponds to the seasons in Indonesia. Based on the graph in Figure 4.7, the months of January to March 2021, September to December 2021, and January to March 2022 had high rainfall in the range of 2-19 mm/day. During these months, Indonesia was experiencing the rainy season. In contrast, the months of April to August in 2021-2022 had low rainfall, with no rainfall detected in August 2021, as it was experiencing the dry season. If we focus on December 2021, that month had relatively high rainfall compared to other months, at 15.12 mm/day. Several months before that, from September to November 2021, also had increasing rainfall. September, October, and November 2021 were already categorized as part of the rainy season. Therefore, the rainfall in the months leading up to and during the eruption had an average value of 7.3 mm/day.

Based on the analysis of the three parameters and the indicators of the causes of the eruption of Mount Semeru in Table 3.5, it can be concluded that the eruption in December 2021 was likely triggered by an external factor (collapse). This is indicated by the decrease in the lava dome's area (morphology), the detection of many thermal anomalies with temperatures greater than 50ºC, and an average rainfall of more than 0 mm/day in several months leading up to the eruption. The correlation between morphology and thermal anomaly area is negative, so when the lava dome's area decreases, there is an increase in the thermal anomaly area. On the other hand, there is no correlation between thermal anomalies and rainfall, but there is an indication of an increase in rainfall along with an increase in the thermal anomaly area in December 2021, as shown in the graph in Figure 4.1. The conditions in December 2021 suggest a decrease in the lava dome's area, an increase in the thermal anomaly area, and an increase in rainfall, which may indicate that the eruption was triggered by a collapse.

In this study, there is also an indication that the anomaly in December 2021 was caused by rainfall. However, due to the very short-lived eruption and collapse, the remote sensing data resolution used in this study may not be sufficient to draw quantitative conclusions about whether rainfall was the cause of the collapse or not. For further research, high temporal resolution satellite data, such as ECOSTRESS, as utilized by Chang et al. (2021) for assessing thermal variations in urban areas using land surface temperature, may be required. High temporal resolution satellite data can also be combined with seismic data to determine the factors contributing to the collapse, whether external or internal, and to obtain detailed information about the timing of the eruption (Walter et al., 2019).

CHAPTER V

CONCLUSION

Observations of Mount Semeru were conducted using remote sensing methods through morphology, thermal, and rainfall parameters in the year 2021-2022. Before the eruption (January-October 2021), there were no significant changes in the extent of the lava dome, but thermal anomalies were detected in certain months. During the eruption in December 2021, there was an 81% decrease in the lava dome's extent, with thermal anomalies detected covering an area of 106,166 square meters, accompanied by pyroclastic flows and ash clouds. Rainfall in December 2021 was relatively high, at 15.12 mm/day. After the eruption (January-December 2022), there was a maximum increase of 49% in the lava dome's extent, and more thermal anomalies were detected compared to 2021. Rainfall before and after the eruption had high values during the rainy season (September-March) and low values during the dry season (April-August).

Based on the analysis of morphology, thermal, and rainfall parameters, rainfall does not show a significant correlation with thermal anomalies. However, there is an indication that in December 2021, there was an increase in rainfall values coinciding with an increase in the extent of thermal anomalies. Additionally, the extent of thermal anomalies shows a negative correlation with the extent of the lava dome. This may indicate that the eruption of Mount Semeru in December 2021 occurred due to external factors (collapse) because of the decreased lava dome extent, increased thermal anomaly extent, and increased rainfall values.

A quantitative conclusion regarding the factors causing the collapse of Mount Semeru cannot be confirmed at this time. However, there are indications of collapse due to external factors, as evidenced by anomalies in rainfall and thermal activity in December 2021. To further investigate the events in December 2021, high-temporal-resolution satellite data would be necessary to determine the impact of rainfall, along with seismic data to monitor magma activity during that month.

BIBLIOGRAPHY

Amani, M., Ghorbanian, A., Ahmadi, S. A., Kakooei, M., Moghimi, A., Mirmazloumi, S. M., Moghaddam, S. H. A., Mahdavi, S., Ghahremanloo, M., Parsian, S., Wu, Q., & Brisco, B. (2020). *Google Earth Engine Cloud Computing Platform for Remote Sensing Big Data Applications: A Comprehensive Review*. IEEE Journal of Selected Topics in Applied Earth Observations and Remote Sensing, 13, 5326-5350, doi: 10.1109/JSTARS.2020.3021052.

Aprillya, S. R. (2021). *Mengapa Gunung Semeru Erupsi? Ini Penjelasan Para Pakar*. Accessed on January 16, 2023, from https://news.detik.com/berita/d-5852454/mengapa-gunung-semeru-erupsi-ini-penjelasan-para-pakar

Araffah, M. R., & Purnama, I. (2020). *Hubungan Motivasi Kerja dengan Produktivitas Pegawai pada Kantor Setda Kabupaten Bima*. Jurnal Manajemen dan Bisnis, 2, 2, 149-156, doi: https://doi.org/10.30812/target.v2i2.747

Aufaristama, M., Hoskuldsson, A., Jonsdottir, I., Ulfarsson, M.O., & Thordarson, T. (2018). *New Insights for Detecting and Deriving Thermal Properties of Lava Flow Using Infrared Satellite during 2014–2015 Effusive Eruption at Holuhraun, Iceland*. Remote Sens., 10, 151. https://doi.org/10.3390/rs10010151

Blackett, M. (2014). *Early Analysis of Landsat-8 Thermal Infrared Sensor Imagery of Volcanic Activity*. Remote Sens. 6, 2282-2295. https://doi.org/10.3390/rs6032282

BMKG. (2022). *Probabilistik Curah Hujan 20 mm (tiap 24 jam)*. Accessed on January 20, 2023, from https://www.bmkg.go.id/cuaca/probabilistik-curah-hujan.bmkg#

Britannica, T. Editors of Encyclopaedia. (2016). *volcanic dome*. Encyclopedia Britannica. https://www.britannica.com/science/volcanic-dome

Chang, Y., Xiao, J., Li, X., Middel, A., Zhang, Y., Gu, Z., Wu, Y., & He, S. (2021). *Exploring diurnal thermal variations in urban local climate zones with ECOSTRESS land surface temperature data*. Remote Sensing of Environment, 263, https://doi.org/10.1016/j.rse.2021.112544

CHC. (2022). *CHIRPS: Rainfall Estimates from Rain Gauge and Satellite Observations*. Accessed on January 18, 2023, from https://chc.ucsb.edu/data/chirps

Earth Engine Data Catalog. (1981). *CHIRPS Daily: Climate Hazards Group InfraRed Precipitation With Station Data (Version 2.0 Final)*. Accessed on January 18, 2023, from https://developers.google.com/earth-engine/datasets/catalog/UCSB-CHG_CHIRPS_DAILY

Earth Engine Data Catalog. (2013). *USGS Landsat 8 Collection 2 Tier 1 Raw Scenes*. Accessed on January 21, 2023, from https://developers.google.com/earth-engine/datasets/catalog/LANDSAT_LC08_C02_T1

Earth Engine Data Catalog. (2015). *Planet & NICFI Basemaps for Tropical Forest Monitoring - Tropical Asia*. Accessed on January 21, 2023, from https://developers.google.com/earth-engine/datasets/catalog/projects_planet-nicfi_assets_basemaps_asia

ESDM. (2023). *Pengenalan Gunungapi*. Accessed on January 18, 2023, from https://www.esdm.go.id/assets/media/content/Pengenalan_Gunung_Api.pdf

Farquharson, J.I., & Amelung, F. (2020). *Extreme rainfall triggered the 2018 rift eruption at Kīlauea Volcano*. Nature 580, 491–495. https://doi.org/10.1038/s41586-020-2172-5

Farquharson J.I., & Amelung F. (2022). *Volcanic hazard exacerbated by future global warming-driven increase in heavy rainfall*. R. Soc. Open Sci. 9: 220275. https://doi.org/10.1098/rsos.220275

Geologi, K. E. (2014). *G. Semeru*. Accessed on January 16, 2023, from https://vsi.esdm.go.id/index.php/gunungapi/data-dasar-gunungapi/533-g-semeru?start=1

Gerstman, B. (2016). *14: Correlation*. California: San Jose State University. https://www.sjsu.edu/faculty/gerstman/StatPrimer/correlation.pdf

Global Volcanism Program. (2022). *Semeru (263300) di [Database] Volcanoes of the World (v. 5.0.0; 1 Nov 2022)*. Distributed by Smithsonian Institution, compiled by Venzke, E. https://doi.org/10.5479/si.GVP.VOTW5-2022.5.0

Gloria. (2021). *Perlu Kombinasi Sejumlah Metode Pengamatan di Gunung Semeru*. Accessed on January 16, 2023, from https://ugm.ac.id/id/berita/22070-perlu-kombinasi-sejumlah-metode-pengamatan-di-gunung-semeru

Hariyono, E., & S, L. (2017). *The Characteristics of Volcanic Eruption in Indonesia. In (Ed.), Volcanoes - Geological and Geophysical Setting, Theoretical Aspects and Numerical Modeling, Applications to Industry and Their Impact on the Human Health*. IntechOpen. https://doi.org/10.5772/intechopen.71449

Hsu, J., Huang, W.-R., Liu, P.-Y., & Li, X. (2021). *Validation of CHIRPS Precipitation Estimates over Taiwanat Multiple Timescales*. Remote Sens., 13, 254. https://doi.org/10.3390/rs13020254

Katalog Inderaja. (2018). *LANDSAT-8 Citra Satelit Resolusi Menengah*. Accessed on January 21, 2023, from https://inderaja-catalog.lapan.go.id/application_data/default/pages/about_Landsat-8.html

KBBI. (2016). *Erupsi*. Accessed on January 18, 2023, from https://kbbi.kemdikbud.go.id/entri/erupsi

Konstantinou, K. I., Perwita, C. A., Maryanto, S., Surono, Budianto, A., & Hendrasto, M. (2013). *Maximal Lyapunov exponent variations of volcanic tremor recorded during explosive and effusive activity at Mt Semeru volcano, Indonesia*, Nonlin. Processes Geophys., 20, 1137–1145, https://doi.org/10.5194/npg-20-1137-2013

Kumar, L., & Mutanga, O. (2019). *Google Earth Engine Applications*. Basel: MDPI, http://www.gisandbeers.com/GeoBazar/Libros/Big%20Data/Google%20Earth%20Engine%20Applications.pdf

Lillesand T.M., R. W. Kiefer, & J. W. Chipman. (2004). *Remote Sensing and Image Interpretation*. Fifth Edition. New York: John Wiley and Sons.

Lim, W., & Lee Y. (2017). *Shoelace Formula: Connecting the Area of a Polygon with Vector Cross Product*. The Mathematics Teacher, 110(8), 631–636. https://doi.org/10.5951/mathteacher.110.8.0631

MAGMA Indonesia. (2021). *Erupsi Freatik*. Accessed on January 18, 2023, from https://magma.esdm.go.id/v1/edukasi/glossary/erupsi-freatik

MAGMA Indonesia. (2021). *Erupsi Magmatik*. Accessed on January 18, 2023, from https://magma.esdm.go.id/v1/edukasi/glossary/erupsi-magmatik

MAGMA Indonesia. (2021). *Phreatomagmatic*. Accessed on January 18, 2023, from https://magma.esdm.go.id/v1/edukasi/glossary/phreatomagmatic#:~:text=Phreatomagmatic%20atau%20erupsi%20freatomagmatik%20adalah,letusan%20freatomagmatik%20mengandung%20magma%20klastik.

Masolele, R. N., Sy, V. D., Marcos, D., Verbesselt, J., Gieseke, F., Mulatu, K. A., Moges, Y., Sebrala, H., Martius, C., & Herold, M. (2022). *Using high-resolution imagery and deep learning to classify land-use following deforestation: a case study in Ethiopia*, GIScience & Remote Sensing, 59:1, 1446-1472, DOI: 10.1080/15481603.2022.2115619

Miranda, V., Pina, P., Heleno, S., Gouhier, M., & Dumont, S. (2022). *Reconstruction of The 2014-2015 Fogo Volcano (Cape Verde) Eruption Through Thermal Remotely Sensed Imagery*. Enschede: University of Twente.

Muhsoni, F. F. (2015). *Penginderaan Jauh (Remote Sensing)*. Madura: UTMPress.

NPS. (2023). *Volcanic Domes*. Accessed on January 21, 2023, from https://www.nps.gov/articles/000/domes.htm#:~:text=Because%20they%20are%20made%20up,small%20volcanoes%20with%20limited%20volume

Permana, A. (2021). *Ahli Vulkanologi ITB Jelaskan Penyebab Erupsi Gunung Semeru*. Accessed on January 16, 2023, from https://www.itb.ac.id/berita/detail/58311/ahli-vulkanologi-itb-jelaskan-penyebab-erupsi-gunung-semeru

Planet Team. (2017). *Planet Application Program Interface: In Space for Life on Earth*. San Francisco: CA. https://api.planet.com

Plank, S., Marchese, F., Genzano, N. et al. (2020). *The short life of the volcanic island New Late'iki (Tonga) analyzed by multi-sensor remote sensing data*. Sci Rep 10, 22293. https://doi.org/10.1038/s41598-020-79261-7

Prasetiawan, T. (2021). *Erupsi Gunung Semeru.* Jakarta: Pusat Penelitian Badan Keahlian Sekretariat Jenderal DPR RI.

Prasetyaningtyas, K. (2021). *Prakiraan Musim Hujan Tahun 2021/2022 di Indonesia* Accessed on January 22, 2023, from https://www.bmkg.go.id/iklim/prakiraan-musim.bmkg?p=prakiraan-musim-hujan-tahun-2021-2022-di-indonesia&tag=prakiraan-musim&lang=ID

Prasetyaningtyas, K. (2021). *Prakiraan Musim Kemarau Tahun 2021 di Indonesia*. Accessed on January 22, 2023, from https://www.bmkg.go.id/iklim/prakiraan-musim.bmkg?p=prakiraan-musim-kemarau-tahun-2021-di-indonesia&tag=prakiraan-musim&lang=ID

Prasetyaningtyas, K. (2022). *Prakiraan Musim Hujan Tahun 2022/2023 di Indonesia*. Accessed on January 22, 2023, from https://www.bmkg.go.id/iklim/prakiraan-musim.bmkg?p=prakiraan-musim-hujan-tahun-2022-2023-di-indonesia&tag=prakiraan-musim&lang=ID

Pura, Y. P. (2022). *Informasi Letusan Gunung Api Semeru*. Accessed on January 16, 2023, from https://magma.esdm.go.id/v1/gunung-api/informasi-letusan/1067/show?signature=7e2545a24f2cfd8afadeeb9bdf4290e69f837051a11c22cd24f9817427fd686c

Rahmawati, N., Rahayu, K. & Yuliasari, S.T. (2021). *Performance of daily satellite-based rainfall in groundwater basin of Merapi Aquifer System, Yogyakarta*. Theor Appl Climatol 146, 173–190. https://doi.org/10.1007/s00704-021-03731-9

Reath, K., Pritchard, M., Poland, M., Delgado, F., Carn, S., Coppola, D., . . . Bagnardi, M. (2018). *Thermal, Deformation, and Degassing Remote Sensing Time Series (CE 2000-2017) at the 47 most Active Volcanoes in Latin America: Implications for Volcanic Systems*. Journal of Geophysical Research: Solid Earth, 124 (https://doi.org/10.1029/2018JB016199), 195-218.

Ridwan, M. (2020). *Prakiraan Musim Hujan Tahun 2020/2021 di Indonesia*. Accessed on January 22, 2023, from https://www.bmkg.go.id/iklim/prakiraan-musim.bmkg?p=prakiraan-musim-hujan-tahun-2020-2021-di-indonesia&tag=prakiraan-musim&lang=ID

Sanderson, R. (2006). *Introduction to Remote Sensing*. Mexico: New Mexico State University.

Seltman, H. (2018). *Chapter 9 Simple Linear Regression*. Pittsburgh: Carnegie Mellon University, https://www.stat.cmu.edu/~hseltman/309/Book/chapter9.pdf

Sugiyono. (2019). *Metode Penelitian Kuantitatif, Kualitatif dan R & D*. Bandung: Alfabeta.

Sutanto. (1994). *Penginderaan Jauh Jilid 1 dan II (Bab 1)*. Yogyakarta: Gadjah Mada University Press.

Suwarsono, Hidayat, Suprapto, T., Prasasti, I., Parwati, & Khomarudin, M. R. (2017). *Detecting the brightness temperature from Landsat-8 thermal infra red scanner preceding the Rinjani strombolian eruption 2015*. AIP Conference Proceedings, 1857, 1. https://doi.org/10.1063/1.4987094

The European Space Agency. (2023). *RapidEye*. Accessed on January 21, 2023, from https://earth.esa.int/eogateway/missions/rapideye

Tienrey, C. (2010). *Lava Domes*. Accessed on January 21, 2023, from https://volcano.oregonstate.edu/lava-domes#:~:text=Lava%20domes%20are%20formed%20by,or%20followed%20by%20explosive%20activity.

USGS. (2022). *How Do Volcanoes Erupt?*. Accessed on January 18, 2023, from https://www.usgs.gov/faqs/how-do-volcanoes-erupt

USGS. (2013). *Landsat 8*. Accessed on January 18, 2023, from https://www.usgs.gov/landsat-missions/landsat-8

Wagner, F.H., Dalagnol, R., Silva-Junior, C.H.L., Carter, G., Ritz, A.L., Hirye, M.C.M., Ometto, J.P.H.B., & Saatchi, S. (2023). *Mapping Tropical Forest Cover and Deforestation with Planet NICFI Satellite Images and Deep Learning in Mato Grosso State (Brazil) from 2015 to 2021*. Remote Sens., 15, 521. https://doi.org/10.3390/rs15020521

Walter, T.R., Haghshenas Haghighi, M., Schneider, F.M. et al. (2019). *Complex hazard cascade culminating in the Anak Krakatau sector collapse*. Nat Commun 10, 4339. https://doi.org/10.1038/s41467-019-12284-5

Warsudi, E. (2022). *Prakiraan Musim Kemarau Tahun 2022 di Indonesia*. Accessed on January 22, 2023, from https://www.bmkg.go.id/iklim/prakiraan-musim.bmkg?p=prakiraan-musim-kemarau-tahun-2022-di-indonesia&tag=prakiraan-musim&lang=ID

Xiang, J., Guo, S., Shi, X., Yu, D., Wei, G., Wen, N., . . . Dai, K. (2022). *Revealing the Morphological Evolution of Krakatau Volcano by Integrating SAR and Optical Remote Sensing Images*. Remote Sens, 14, 1399 (https://doi.org/10.3390/rs14061399), 1-11.

Yuliara, I. M. (2016). *Modul Regresi Linier Sederhana*. Bali: Universitas Udayana, https://simdos.unud.ac.id/uploads/file_pendidikan_1_dir/3218126438990fa0771ddb555f70be42.pdf